



nilu

NILU report

Air quality in Sandefjord, Norway

November 2021 – August 2023

NILU report 1/2024		ISBN: 978-82-425-3145-2 ISSN: 2464-3327	CLASSIFICATION: A – Unclassified (open report)
DATE 26.01.2024	SIGNATURE OF RESPONSIBLE PERSON Britt Ann K. Høiskar, forskningsdirektør (sign.)		NUMBER OF PAGES 51
TITLE Air quality in Sandefjord, Norway November 2021 – August 2023			PROJECT LEADER Nuria Castell
			NILU PROJECT NO. O-121139
AUTHOR(S) Vasileios Salamalikis, Núria Castell			QUALITY CONTROLLER Claudia Hak
REPORT PREPARED FOR Sandefjord kommune			CONTRACT REF. Ole Jakob Hansen
ABSTRACT <p>This report examines the air quality patterns in terms of particulate matter with a diameter less than 2.5 µm (PM_{2.5}) in Sandefjord, Norway. PM_{2.5} was monitored through five low-cost sensors in hourly resolution from November 2021 to August 2023. The sensors’ reliability is high, with consistent PM_{2.5} measurements and similar variation over time. Occasional extreme PM_{2.5} was attributed to local contributions with higher values observed during cold months, or specific long-range transport events. Overall, Sandefjord maintained good air quality for most of the measurement period with daily PM_{2.5} levels below the air quality criteria. Residential heating activities (wood burning) is the most significant local source, being more pronounced during winter.</p>			
NORWEGIAN TITLE Luftkvalitet i Sandefjord, Norge			
KEYWORDS PM _{2.5} low-cost sensorsair quality			
ABSTRACT (in Norwegian) <p>Rapporten gir en omfattende analyse av PM_{2.5} - konsentrasjonen i Sandefjord, Norge. I 2021 ble det etablert et målenettverk for PM_{2.5} bestående av fem rimelige luftkvalitetssensorer (LCS). Her gjøres en analyse av målte PM_{2.5}-konsentrasjoner i perioden november 2021 til august 2023. Lignende variasjon og PM_{2.5}-målinger som er konsistente over tid indikerer høy sensorpålitelighet. En og annen ekstrem PM_{2.5} ble tilskrevet lokale bidrag med høyere verdier observert i kalde måneder, eller spesifikke episoder med langtransportert luftforurensning. Samlet sett var det god luftkvalitet i Sandefjord i det meste av måleperioden med PM_{2.5}-nivåer under grenseverdiene. Utslipp fra vedfyring er den viktigste lokale kilden, og er mer uttalt om vinteren.</p>			
PUBLICATION TYPE: Digital document (pdf)		COVER PICTURE: Source: NILU	

© Stiftelsen NILU

Citation: Salamalikis, V, Castell, N. (2023). Air quality in Sandefjord, Norway. November 2021 – August 2023. (NILU report 1/2024). Kjeller: NILU.

NILU's ISO Certifications: NS-EN ISO 9001 and NS-EN ISO 14001. NILU's Accreditation: NS-EN ISO/IEC 17025.

Contents

Contents	4
Executive summary	5
Sammendrag (norsk)	7
1 General aspects.....	9
2 Air quality sensor network in Sandefjord	9
2.1 The nearest reference site	10
2.2 Comparison with reference instrument: distant-based approach	11
3 Air quality guidelines and limit values.....	11
4 PM_{2.5} distribution	12
4.1 PM _{2.5} at Tønsberg station.....	12
4.2 Distant-based comparison of sensors against reference station	15
4.3 Distribution of PM _{2.5} in Sandefjord using sensors	18
4.3.1 Hourly variation and sensor-to-sensor intercomparison.....	18
4.3.2 Daily and weekly variation	20
4.3.3 Monthly and seasonal variation.....	24
4.3.4 Yearly variation	26
4.3.5 Diurnal variation.....	27
4.3.6 PM _{2.5} vs. air temperature – a proxy for residential heating.....	31
5 Local and regional sources.....	34
6 Results in relation to the limit values and Air Quality Criteria	37
7 General conclusions	40
8 References.....	41
Appendix A	43

Executive summary

Many urban areas in Europe face significant challenges related to outdoor air quality, with implications for public health, environmental sustainability, and overall quality of life. Among the various atmospheric pollutants, air particulates with a diameter less than $2.5\ \mu\text{m}$ ($\text{PM}_{2.5}$) with natural or anthropogenic origin, are of critical concern because of their linkage to diverse health effects. The primary local sources of $\text{PM}_{2.5}$ in urban areas are combustion (vehicle engines and residential heating) and secondary particle formation.

On the other side, regional sources including particles generated at distant areas and transported by the wind and biogenic originated particles from wildfires, dust intrusions or other environmental phenomena may also contribute to the observed $\text{PM}_{2.5}$ concentrations over a specific urban setting.

The advances on the Internet of Things (IoT) coupled with the development of low-cost air sensors enable the creation of local-scale air quality monitoring networks and can to a certain degree enhance already existing regulatory networks for monitoring air quality. Low-cost sensors cannot replace reference instruments, but may act in a complementary manner, providing insightful information about air quality patterns within a specific area.

It is important to highlight that low-cost sensors do not fulfil the requirements for equivalence with the reference method and that sensor measurements cannot be evaluated with respect to legally binding limit values. Low-cost sensors may be used for indicative measurements and to compare local spatial differences of the $\text{PM}_{2.5}$ levels.

This report aims to provide a comprehensive analysis of the $\text{PM}_{2.5}$ air quality patterns in Sandefjord, southern Norway. The air quality monitoring network comprises five low-cost air quality sensors (LCS). The closest official air pollution monitoring station is situated in Tønsberg (~18 km from Sandefjord). $\text{PM}_{2.5}$ concentrations are analyzed from November 2021 to August 2023. The main topics addressed in this report are outlined as:

- $\text{PM}_{2.5}$ variability on different temporal scales
- Diurnal variation of $\text{PM}_{2.5}$ and discussion of possible local emissions
- Linkage of $\text{PM}_{2.5}$ with air temperature as an effort to discuss the contribution of residential heating
- Effect of local and regional sources on $\text{PM}_{2.5}$ concentrations

Broadly, the report suggests that $\text{PM}_{2.5}$ low-cost sensors can already provide valuable qualitative information about air quality in Sandefjord since no other reference measurements are available in the area. The key findings can be summarized as follows:

- Similar variations and consistent over time $\text{PM}_{2.5}$ measurements indicate high sensor reliability. The hourly average $\text{PM}_{2.5}$ level, averaged for 5 sensors, extends from 5.9 to $8\ \mu\text{g m}^{-3}$. Elevated $\text{PM}_{2.5}$ concentrations are attributed to local contributions, or specific PM episodes. Seasonal variations are evident, with $\text{PM}_{2.5}$ concentration exhibiting higher values during cold months. $\text{PM}_{2.5}$ in urban areas of Sandefjord is higher within the urban area than in Stokke because of different local emission sources.
- The diurnal distribution of $\text{PM}_{2.5}$ shows a typical urban profile, exhibiting a bimodal pattern with two notable peaks. The significance and magnitude of the observed peaks are controlled by:
 - a. the time of day that peak occurs. For instance, the observed morning peak is lower than the evening peak.
 - b. the season. In summer, the diurnal $\text{PM}_{2.5}$ pattern is nearly flat because of the minimal local emissions while more discernable peaks within the day are documented in winter.
 - c. the magnitude of local sources.

- PM_{2.5} is well correlated with air temperature during specific months (November to March) and hours of the day (15:00-23:00). An increase in PM_{2.5} during lower temperature conditions suggests the dominance of residential heating-based activities.

Local sources account for more than 50% of PM_{2.5}, during the cold winter months when emission from woodburning is an important local source for air pollution (e.g. elevated concentrations in December 2021 and 2022).

- The air quality in Sandefjord is good during most of the year, with levels of daily mean averages of PM_{2.5} below the air quality criteria (Luftkvalitetskriteriene). Daily mean averages of PM_{2.5} above the air quality criteria (15 µg m⁻³) are mainly observed during the winter months. However, it is important to highlight that sensors suffer from biases and are not able to provide the same accuracy as reference instrumentation. The number of exceedances of the daily air quality criteria observed by the sensors can only be understood as an indication that in winter there might be a moderate health risk for the population due to air pollution levels.
- The sensor network was also able to capture a regional transport event in March 2022 that caused high levels of air pollution.
- All air quality sensors in Sandefjord area report values for 2022 lower than the annual legal limit value of 10 µg m⁻³ given in "forurensningsforskriften". However, the annual concentrations are above the lower assessment threshold of 5 µg m⁻³, which coincides with the revised air quality criterion for PM_{2.5} annual average, and lower or close to the upper assessment threshold.

Sammendrag (norsk)

Mange byer og tettsteder i Europa står overfor betydelige utfordringer knyttet til utendørs luftkvalitet, noe som påvirker folkehelse, miljømessig bærekraft og generell livskvalitet. Blant de ulike typene luftforurensning er svevestøvpartikler med en diameter mindre enn 2.5 mikrometer ($PM_{2.5}$) til stor bekymring. Det er fordi disse partiklene, som kan ha både naturlige og menneskeskapte kilder, kan knyttes til ulike negative helseeffekter. De primære lokale kildene til $PM_{2.5}$ i urbane områder er utslipp fra kjøretøy (eksosutslipp, dannelse av veistøv på grunn av mekanisk slitasje fra dekk og bremses samt oppvirvling av veistøv), industrivirksomhet og oppvarming av boliger (vedfyring). Sistnevnte gjelder hovedsaklig i den kalde årstiden.

Regionale kilder kan også bidra til de målte $PM_{2.5}$ -konsentrasjonene i urbane områder. Dette inkluderer partikler som transporteres hit med vinden fra kilder langt borte. I tillegg kan partikler med naturlige kilder som skogbranner, lokalt- eller langtransportert svevestøv og andre miljøfenomener også bidra til $PM_{2.5}$ -konsentrasjonene i norske byer og tettsteder.

Fremskrittene de senere årene innen tingenes internett (Internet of Things, IoT) kombinert med utviklingen av rimeligere luftkvalitetssensorer, gjør det mulig å etablere et nettverk av luftkvalitetssensorer for overvåkning av luftkvalitet på lokalt nivå. Samme teknologier kan også brukes til å i noen grad forbedre de allerede eksisterende målenettverkene. Lavkostsensorer kan likevel ikke erstatte referansemåleinstrumentene. Førstnevnte fungerer hovedsakelig utfyllende, og gir nyttig innsikt i luftkvalitetsmønstre innen et gitt område.

Det er viktig å fremheve at lavkostsensorer heller ikke oppfyller kravene til ekvivalens med referansemetoden for måling av $PM_{2.5}$. Slike lavkostsensormålinger kan derfor ikke benyttes for å vurdere luftkvaliteten opp mot juridisk bindende grenseverdier gitt i forurensningsforskriften. Lavkostsensorer kan derimot brukes til å utføre veiledende målinger og for å sammenligne lokale forskjeller på $PM_{2.5}$ -nivåer.

Rapporten har som mål å gi en omfattende analyse av $PM_{2.5}$ variasjonen i Sandefjord, Sør-Norge. Det er etablert et målenettverk for luftkvalitet bestående av fem rimelige luftkvalitetssensorer (LCS). Nærmeste offisielle målestasjon for luftkvalitet ligger i Tønsberg (~18 km fra Sandefjord). Her gjøres en analyse av målte $PM_{2.5}$ -konsentrasjoner i perioden november 2021 til august 2023. Hovedtemaene som tas opp i denne rapporten er:

- Studere tidsvariasjoner av $PM_{2.5}$ over timer, døgn og år
- Se om døgnvariasjon av $PM_{2.5}$ kan gi informasjon om mulige lokale utslipp
- Se om koblingen mellom $PM_{2.5}$ og lufttemperatur gir informasjon om bidraget fra vedfyring til $PM_{2.5}$ -konsentrasjoner
- Effekt av lokale og regionale kilder på $PM_{2.5}$ -konsentrasjoner

Resultatene som presenteres i rapporten viser at $PM_{2.5}$ lavprissensorer kan gi verdifull kvalitativ informasjon om luftkvaliteten i Sandefjord siden ingen andre referansemålinger er tilgjengelige i området. De viktigste funnene i rapporten kan oppsummeres som følger:

- Lignende variasjon og $PM_{2.5}$ -målinger som er konsistente over tid indikerer høy sensorpålitelighet. Gjennomsnittlig timemiddel for $PM_{2.5}$, beregnet for de 5 sensorene, varierer fra 5,9 til 8 $\mu\text{g}/\text{m}^3$. Forhøyede $PM_{2.5}$ -konsentrasjoner tilskrives lokale bidrag, eller spesifikke PM-episoder. Det observeres tydelige sesongvariasjoner, med høyere $PM_{2.5}$ -konsentrasjon i de kalde månedene. $PM_{2.5}$ i Sandefjord er høyere innenfor sentrum enn i Stokke på grunn av ulike lokale utslippskilder.
- Døgnvariasjonen av $PM_{2.5}$ viser en typisk urban profil, og har et bimodalt mønster med to tydelige topper. Betydningen og størrelsen på de observerte toppene styres av:

- a) tidspunktet på dagen toppen inntreffer. For eksempel er den observerte morgentoppen lavere enn kveldstoppen.
 - b) sesongen. Om sommeren varierer $PM_{2,5}$ -konsentrasjonen svært lite over døgnet på grunn av lave lokale utslipp, mens det observeres mer merkbare topper i konsentrasjonen i løpet av dagen om vinteren.
 - c) omfanget av lokale kilder.
- $PM_{2,5}$ er godt korrelert med lufttemperaturen i enkelte måneder (november til mars) og i enkelte timer på døgnet (15:00-23:00). En økning i $PM_{2,5}$ ved lave temperaturer antyder at utslipp fra oppvarming (vedfyring) er en dominerende kilde.

Lokale kilder står for mer enn 50 % av $PM_{2,5}$ i de kalde vintermånedene når utslipp fra vedfyring er en viktig lokal kilde til luftforurensning (f.eks. forhøyede konsentrasjoner i desember 2021 og 2022).

- Luftkvaliteten i Sandefjord er god store deler av året, med døgnmiddelverdier av $PM_{2,5}$ under anbefalte nivåer gitt i Luftkvalitetskriteriene. Døgnmiddelverdier over luftkvalitetskriteriet på $15 \mu\text{g m}^{-3}$ ble hovedsakelig observert i vintermånedene. Det er viktig å fremheve at disse rimelige sensorene ikke er i stand til å gi samme nøyaktige målinger som referanseinstrumenter. Antall overskridelser av luftkvalitetskriteriet bør derfor kun forstås som en indikasjon på at høy luftforurensning kan utgjøre moderat helserisiko for befolkningen i vintermånedene.
- Sensornettverket klarte å fange opp en episode med langtransportert luftforurensning i mars 2022 som forårsaket høye nivåer av luftforurensning.
- Alle luftkvalitetssensorer i Sandefjord-området rapporterer verdier lavere enn grenseverdien gitt i forurensningsforskriften for årsmiddel av $PM_{2,5}$ på $10 \mu\text{g m}^{-3}$. De årlige konsentrasjonene er imidlertid over nedre vurderingsterskel i Forurensningsforskriften på $5 \mu\text{g m}^{-3}$ som nå er sammenfallende med anbefalt nivå i nye luftkvalitetskriterier, men lavere eller nær den øvre vurderingsterskelen.

Air quality in Sandefjord, Norway

November 2021–August 2023

1 General aspects

A dense air quality network plays a pivotal role in the monitoring of air quality over a geographical region. It enables the comprehensive evaluation of atmospheric pollutants in various settings, and it is crucial not only for scrutinizing areas characterized by prominent emission sources and elevated air pollutant concentrations ('hot spots') but also for examining areas that experience lower human-induced contributions ('background locations'). Extensive monitoring, conducted at fine spatiotemporal scales, can offer valuable information on processes, emission sources, and air quality levels within a study area.

Particulate matter (PM) is a major atmospheric pollutant, which comprises inorganic and organic components from various natural and anthropogenic sources. Particulate matter with a diameter less than $2.5\ \mu\text{m}$ ($\text{PM}_{2.5}$) is well-recognized for its direct and indirect effects on both local and global climate, as well as its impact on human health. In Norway, primary sources of local air pollution in cities and towns stem mainly from road traffic and residential heating. Other sources are industrial activities and maritime traffic. Various city networks have been established across Norway to investigate local based air pollution.

Recent advancements in low-cost technologies now make it possible to establish local-scale networks for monitoring air quality, providing valuable insights into air quality patterns within specific areas. These low-cost instruments, while of suboptimal quality, can offer insights into nearby sources of pollution, complement existing air quality networks, establish new ones, and enhance our understanding of pollutant concentrations, their origins, and their direct linkages to local climate and public health. In contrast, regulatory monitoring systems (i.e. equipped, operated and located according to requirements given in the Air Quality Directive/Forurensningsforskriften), provide the highest level of accuracy and deliver reliable, high-quality data in urban environments. The purpose of the official stations is not to measure full spatial coverage, but to measure air pollution at the worst spots in a city. Particularly in regions lacking or having limited regulatory monitoring, low-cost air quality sensors serve as an alternative solution for conveniently collecting data at fine spatiotemporal scales and addressing air quality concerns. Low-cost sensors provide indicative measurements and can be used to compare local differences of the $\text{PM}_{2.5}$ level. However, it is important to mention that low-cost sensors cannot be utilized for regulatory assessments.

The primary objective of this report is to assess and communicate the indicative levels of air pollution, specifically $\text{PM}_{2.5}$, in Sandefjord, Norway. These measurements are crucial for understanding air quality patterns across different timescales within the study area and gaining a broad understanding of local and regional contributions to $\text{PM}_{2.5}$ concentrations.

2 Air quality sensor network in Sandefjord

The air quality monitoring network in Sandefjord comprised five low-cost air quality sensors (LCS). Outdoor air quality was assessed using Airly sensors (<https://airly.org/en>). The Airly sensor system incorporates a Plantower PMS5003 sensor (https://www.plantower.com/en/products_33/74.html), which uses laser-based light scattering for measuring airborne particles with aerodynamic diameters ranging from 0.3 to $10\ \mu\text{m}$. Particulate matter (PM) mass concentrations are provided for three different sizes, $<1\ \mu\text{m}$ (PM_{10}), $<2.5\ \mu\text{m}$ ($\text{PM}_{2.5}$), and $<10\ \mu\text{m}$ (PM_{10}), expressed in micrograms per cubic meter ($\mu\text{g m}^{-3}$). According to the manufacturer, the measurement range is 0 – $1000\ \mu\text{g m}^{-3}$ with a claimed accuracy of $\pm 1\ \mu\text{g m}^{-3}$ for $\text{PM}_{2.5}$. In addition to PM, the Airly system also records basic

meteorological data such as air temperature ($^{\circ}\text{C}$), humidity (%), and air pressure (hPa). The data provided have hourly temporal resolution. However, several intercomparison studies have shown that PM_{10} from LCSs differs significantly from measurements of regulatory instruments, indicating that LCS are not useful for monitoring coarse particles.

Figure 1 illustrates the geographical arrangement of the LCS units (represented by blue symbols), with three of the sensors situated in close proximity to the port, one located approximately 1 km away from the port, and the fifth sensor (ID450) is positioned in the municipality of Stokke, approximately 11 km from Sandefjord city. It is noted that there is no site classification for the low-cost sensors.

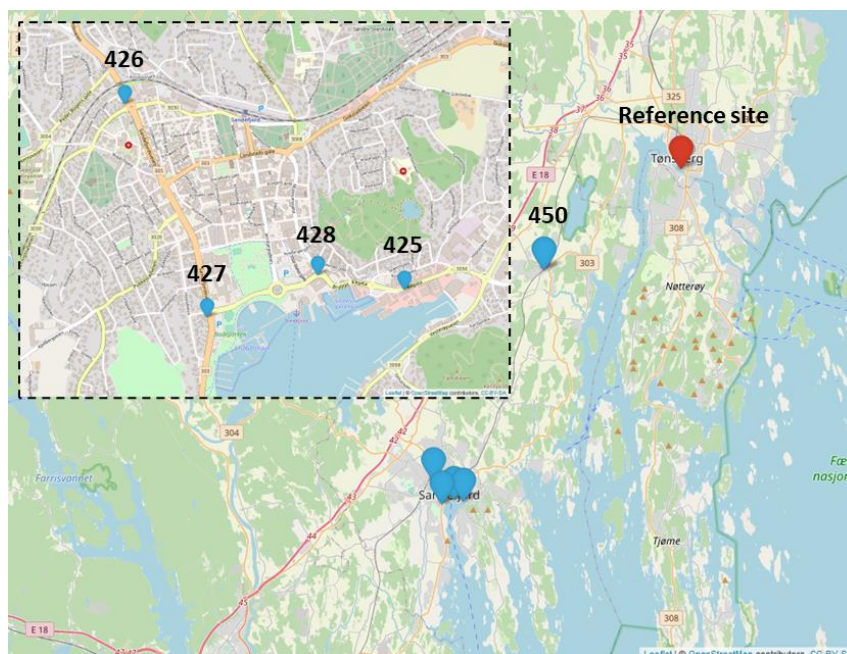


Figure 1: Air quality sensors deployed in Sandefjord, with the red marker denoting the nearest reference station located in Tønsberg. The inset illustrates the sensors positioned within the urban area.

The sensor network became fully operational in November 2021, with the addition of sensor ID450 in December 2021. The data completeness map displayed in Figure A1 indicates sufficient data coverage, with only a few instances of missing data.

2.1 The nearest reference site

The nearest official air pollution monitoring station is situated in Tønsberg, located approximately 18 km from Sandefjord, denoted by the red symbol in Figure 1. This station monitors traffic-related air quality in the central area of Tønsberg and shares information on luftkvalitet.nilu.no. Historical data can be accessed through the following link: <https://luftkvalitet.nilu.no/en/historical>. The station monitors PM_{10} , $\text{PM}_{2.5}$, PM_{10} , NO , and NO_2 , and it offers data with an hourly resolution. In this report, the analysis of $\text{PM}_{2.5}$ data spans from November 2021 to August 2023. This time frame has been selected to ensure temporal consistency with the operational period of Sandefjord's air quality network.

2.2 Comparison with reference instrument: distant-based approach

A calibration procedure necessitates the use of high-quality instruments that are ideally situated close to the low-cost air quality sensors or, in the best-case scenario, collocated with some of them for a significant duration. However, when reference instruments are not readily available in close proximity, a distant-based validation approach provides an alternative means to assess the sensors' performance. Specifically, air quality sensors can be compared to reference data for specific time intervals, particularly during periods when air quality conditions are favorable, characterized by low PM_{2.5} concentrations ([1], [2]).

It is worth noting that relative humidity also plays a role in influencing PM_{2.5} levels. In a local scale, high relative humidity conditions have an effect to reduce resuspension of particles. In general, water vapor molecules interact with aerosol particles, modifying their size, chemical composition, optical properties, and more. The increase in particle diameter due to water uptake is known as hygroscopic growth, and this effect is more noticeable under high relative humidity conditions ([3], [4], [5]). Given this understanding, it is possible to correct LCS PM_{2.5} readings using a humidity-based algorithm based on the κ-Köhler theory ([4], [5])

$$\frac{LCS PM_{2.5}}{Reference PM_{2.5}} = 1 + \frac{\frac{\rho_w}{\rho_p} \kappa}{-1 + \frac{1}{a_w}} \quad Eq. 1$$

with κ: the hygroscopic growth factor, ρ_w: the water density, which is equal to 1 µg m⁻³, ρ_p: the particle's density, which is equal to 1.65 µg m⁻³, and α_w: the water activity, expressed as (RH/100), where RH is the relative humidity in percent.

Typically, the hygroscopic growth parameter κ is estimated through a humidogram, which is the ratio of dry particle mass to wet particle mass against water activity, using a non-linear regression. However, in cases where the reference instrument is not collocated with the low-cost sensors, estimating κ based on the humidogram could potentially lead to erroneous results. Finally, κ is set to a fixed value of 0.4 following [6].

3 Air quality guidelines and limit values

Humans can be adversely affected by exposure to air pollutants in ambient air. National and international limit and guideline values and air quality objectives have therefore been established for a number of pollutants present in the air.

The limit, threshold and guideline values for PM_{2.5} are summarised in Table 1. They apply over differing periods of time because the observed health impacts associated with PM_{2.5} occur over different exposure times. Limit values (Forurensningsforskriften¹) are legally binding. In case of exceedances, authorities must develop and implement air quality management plans which should aim to bring concentrations of air pollutants to levels below the limit and target values.

The Norwegian Environment Agency and the Institute of Public Health have developed Air Quality Criteria (Luftkvalitetskriterier²) that are set for the protection of health and are generally stricter than the comparable limit values. The Air Quality Criteria are based on existing knowledge about the potential health effects of exposure to air pollution. The criteria are set at a level that most people can be exposed to without experiencing harmful health effects. The Air Quality Criteria are recommendations and not legally binding. The Air Quality Criteria has recently been up-dated

¹ [Forskrift om begrensning av forurensning \(forurensningsforskriften\) - Del 3. Lokal luftkvalitet - Lovdata](#)

² [Reviderte luftkvalitetskriterier - FHI](#)

(November 2023) and the recommendation for annual mean $PM_{2.5}$ has been reduced from $8 \mu\text{g}/\text{m}^3$ to $5 \mu\text{g}/\text{m}^3$.





Table 1: National limit values and Air Quality Criteria for $PM_{2.5}$.

Compound	Averaging period	Limit value (FF)	Air Quality Criteria (LKK)
$PM_{2.5}$	Day (24 hours)		$15 \mu\text{g m}^{-3}$
	Calendar year	$10 \mu\text{g m}^{-3}$	$5 \mu\text{g m}^{-3}$

The Norwegian Road Administration, the Directorate of Roads, the Directorate of Health, the Institute of Public Health, and the Directorate of the Environment classify air pollutants based on their concentrations and directly relate them to health advisories³. These levels are used in the daily forecasting of air pollution to the public.

Table 2 displays the pollution classes for $PM_{2.5}$ and their respective color-code, named as Air Quality Index (AQI), and the respective ranges. AQI ranges pollution from “Low” for $PM_{2.5}$ below $15 \mu\text{g m}^{-3}$, and it transitions from “Moderate” to “Very High” for concentrations above this threshold. This color-based classification of air quality offers a practical and easily understandable way to disseminate air quality conditions and the associated health effects and provides guidance for the public.

Table 2: Air Quality Index – Air pollution classes for $PM_{2.5}$

Class	Level	Health Risk	$PM_{2.5}$ Day ($\mu\text{g}/\text{m}^3$)
	Low	Small	< 15
	Moderate	Moderate	15 – 25
	High	Considerable	25 – 75
	Very High	Serious	> 75

4 $PM_{2.5}$ distribution

4.1 $PM_{2.5}$ at Tønsberg station

Figure 2 illustrates the temporal distribution of $PM_{2.5}$ data at the nearest reference station in Tønsberg on an hourly, daily, and monthly basis. The hourly $PM_{2.5}$ concentrations ranged from 0.1 to $65.4 \mu\text{g m}^{-3}$, with an average concentration of $6.6 \pm 5.7 \mu\text{g m}^{-3}$ (mean \pm standard deviation). In Figure 2a, colored horizontal lines correspond to different percentiles of the hourly $PM_{2.5}$ data, such as 5%: $1.3 \mu\text{g m}^{-3}$, 25%: $2.9 \mu\text{g m}^{-3}$, 50%: $4.9 \mu\text{g m}^{-3}$, 75%: $8.5 \mu\text{g m}^{-3}$, and 95%: $17.3 \mu\text{g m}^{-3}$. Notably, peak $PM_{2.5}$ concentrations are observed in the upper 5% of the data, are mainly associated with local emissions or specific particulate matter events. The seasonal distribution is evident in the $PM_{2.5}$ hourly time series, with higher concentrations observed during the colder months.

³

https://luftkvalitet.miljodirektoratet.no/artikkel/artikler/helserad_og_forurensningsklasser/#Forurensningsklasser

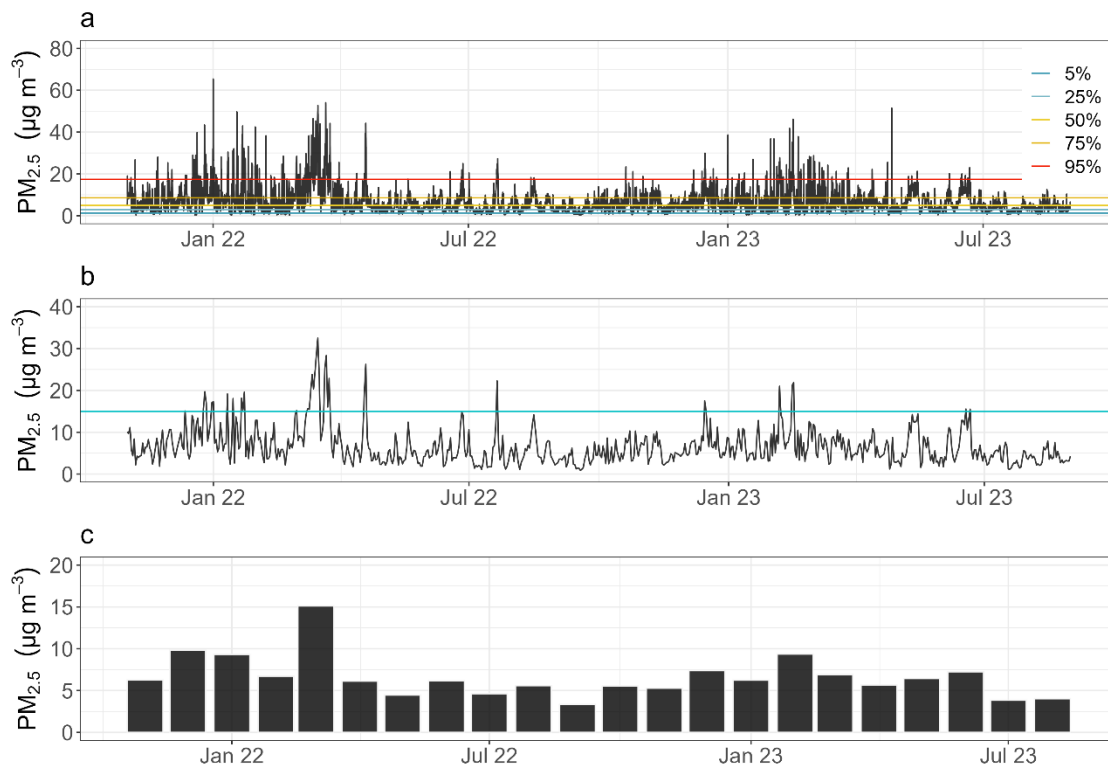


Figure 2: Time series of a) hourly, b) daily (24-h averaged) and c) monthly PM_{2.5} at the Tønsberg reference site. The vertical axis label is in units of µg m⁻³. The colored lines in the upper panel are the 5%, 25%, 50%, 75%, and 95% percentiles of PM_{2.5}. The horizontal blue line in the middle panel denotes the national PM_{2.5} guideline for daily averages of 15 µg m⁻³.

A similar pattern emerges in the daily variation of PM_{2.5}, as shown in Figure 2b. The daily average (± 1 standard deviation) PM_{2.5} concentration is 6.6 ± 4.4 µg m⁻³, and the range of the daily concentrations extends from 0.8 to 32.5 µg m⁻³. Monthly PM_{2.5} data, displayed in Figure 2c, smooth out the variability seen in daily measurements and range between 3.3 to 15.1 µg m⁻³. Seasonal variation is apparent, with higher concentrations during winter months compared to summer. Notably, the highest monthly PM_{2.5} is observed in March 2022, significantly deviating from other months.

Analysis of the hourly and daily PM_{2.5} time series reveals sustained elevated concentrations throughout March 2022. This unusual pattern is attributed to a PM pollution episode impacting Europe ([8],[9]). The episode is characterized as complex and dynamic, involving contributions from various sources, including residential heating, traffic emissions, wildfires, and North African desert dust intrusions ([8],[9]).

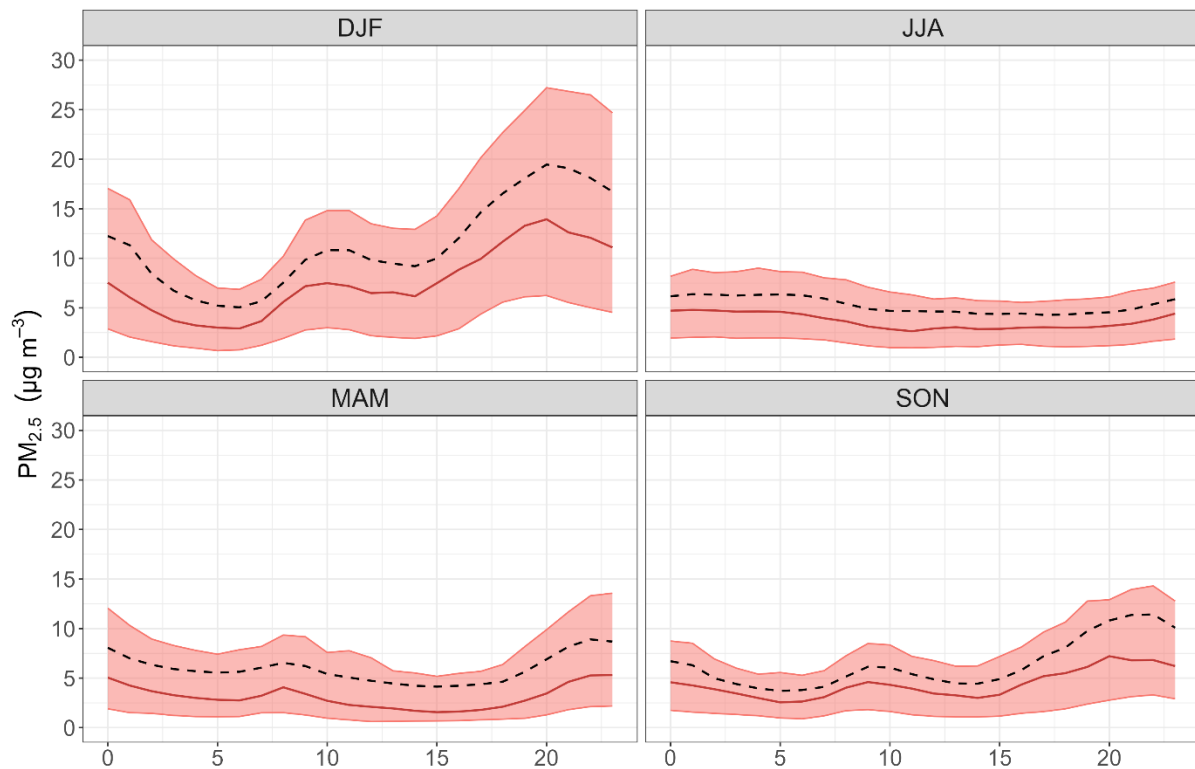


Figure 3: Diurnal variation of $PM_{2.5}$ at Tønsberg reference station. The vertical axis label is in units of $\mu\text{g m}^{-3}$. The solid red and dashed black lines are for the median and average $PM_{2.5}$, respectively. The shaded area corresponds to the interquartile range, $IQR = Q_{75\%} - Q_{25\%}$, with $Q_{X\%}$ the $X\%$ percentile of the data. The header in each panel represents the season with DJF – Winter (December, January, February), MAM – Spring (March, April, May), JJA – Summer (June, July, August) and SON – Autumn (September, October, November).

The diurnal variation of $PM_{2.5}$ shows a typical urban profile (Figure 3). The diurnal profile is affected by various factors, including emissions, meteorological conditions, and anthropogenic activities. Generally, $PM_{2.5}$ during the day exhibits a distinct pattern, with higher concentrations during specific times of the day. The patterns and the magnitude of the concentrations depend on the location and the local factors — this is discussed in detail below.

In summer, $PM_{2.5}$ remains relatively stable throughout the day, ranging from 4.2 to $6.4 \mu\text{g m}^{-3}$, with a daily average of $5.2 \mu\text{g m}^{-3}$. It is mainly attributed to the effective dispersion of air pollutants during the summer period and the large vertical movements of air masses. Also, local emissions such as residential heating are absent during the season. In contrast, $PM_{2.5}$ levels in the other seasons follow a bimodal pattern, characterized by two distinct peaks. The first peak occurs from 08:00 to 11:00 and is dominated by traffic, vehicular emissions. The second peak takes place from 19:00 to 22:00 and is influenced by both traffic and other sources such as residential heating and the lower boundary layer height at night. This pattern is most prominent in winter, as depicted in the upper left panel of Figure 3. In addition to local emissions, meteorological phenomena like temperature inversions play a significant role in elevating $PM_{2.5}$ levels during winter. A temperature inversion occurs when the air temperature increases with altitude, resulting in warmer air sitting above cooler air, which is a very stable atmospheric state. Warm air acts as a "cap," hindering the vertical mixing of air. This phenomenon keeps air pollutants near the ground, leading to high concentrations and poor air quality conditions. Temperature inversions are particularly prevalent during cloudless winter nights, as the prolonged cooling of surface air facilitates their development.

The hourly average $\text{PM}_{2.5}$ (indicated by dashed black lines in Figure 3) ranges per season are as follows: $5 \mu\text{g m}^{-3}$ to $19.5 \mu\text{g m}^{-3}$ in winter, $4.1 \mu\text{g m}^{-3}$ to $8.9 \mu\text{g m}^{-3}$ in spring, and $3.7 \mu\text{g m}^{-3}$ to $11.4 \mu\text{g m}^{-3}$ in autumn. During both spring and autumn, the evening peak in $\text{PM}_{2.5}$ concentrations is more pronounced than the morning peak.

4.2 Distant-based comparison of sensors against reference station

According to Figure 3, $\text{PM}_{2.5}$ levels between 03:00 and 07:00 are lower compared to other time periods, suggesting a minimal contribution from anthropogenic sources and it is assumed that $\text{PM}_{2.5}$ concentrations are close approximate background levels. During this time window, it is anticipated that $\text{PM}_{2.5}$ data from the air quality sensors closely mirror the variations observed at the reference site.

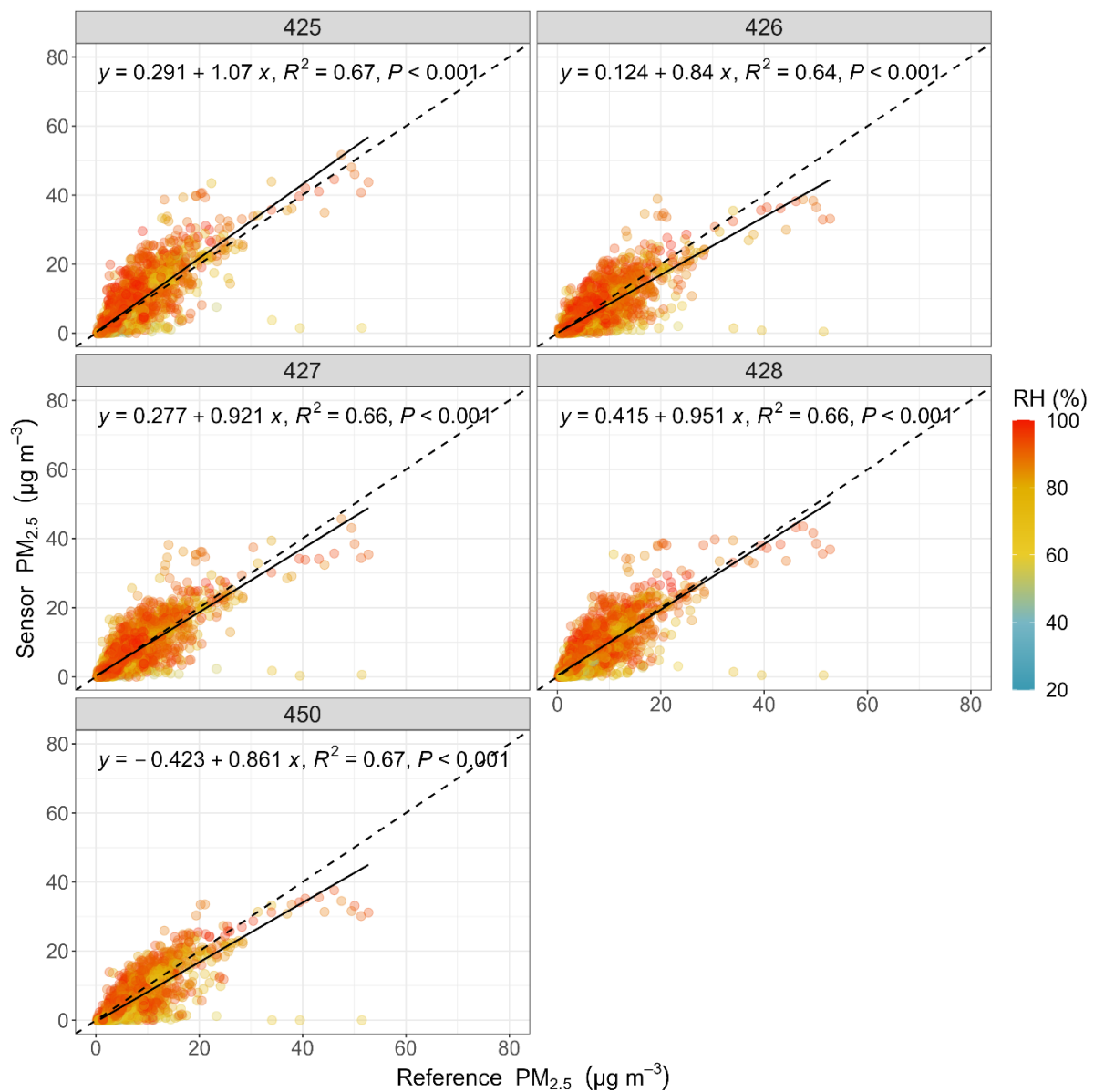


Figure 4: LCS against reference $PM_{2.5}$ at 03:00 – 07:00. Axis labels are in units of $\mu g m^{-3}$. The dashed and solid lines indicate the 1:1 reference line and best linear fit. The equations inside the panels represent the best linear fit, where R^2 is the coefficient of determination and P denotes the statistical significance of the linear fit. If $P < 0.05$, the linear model is significant under the 95% confidence level. Points are colored in terms of relative humidity (in %).

The low-cost sensors exhibited a strong agreement with the reference instrument in Tønsberg during the timeframe from 03:00 to 07:00 (Figure 4). The coefficient of determination (R^2) for this period falls within the range of 0.64 to 0.67. Approximately 30% of the variation that remains unexplained is attributed to measurement uncertainties and local phenomena. The regression slopes, ranging from 0.86 to 1.1, suggest that the low-cost sensors generally tracked the actual observed $PM_{2.5}$ concentrations during the hours when pollution levels are low.

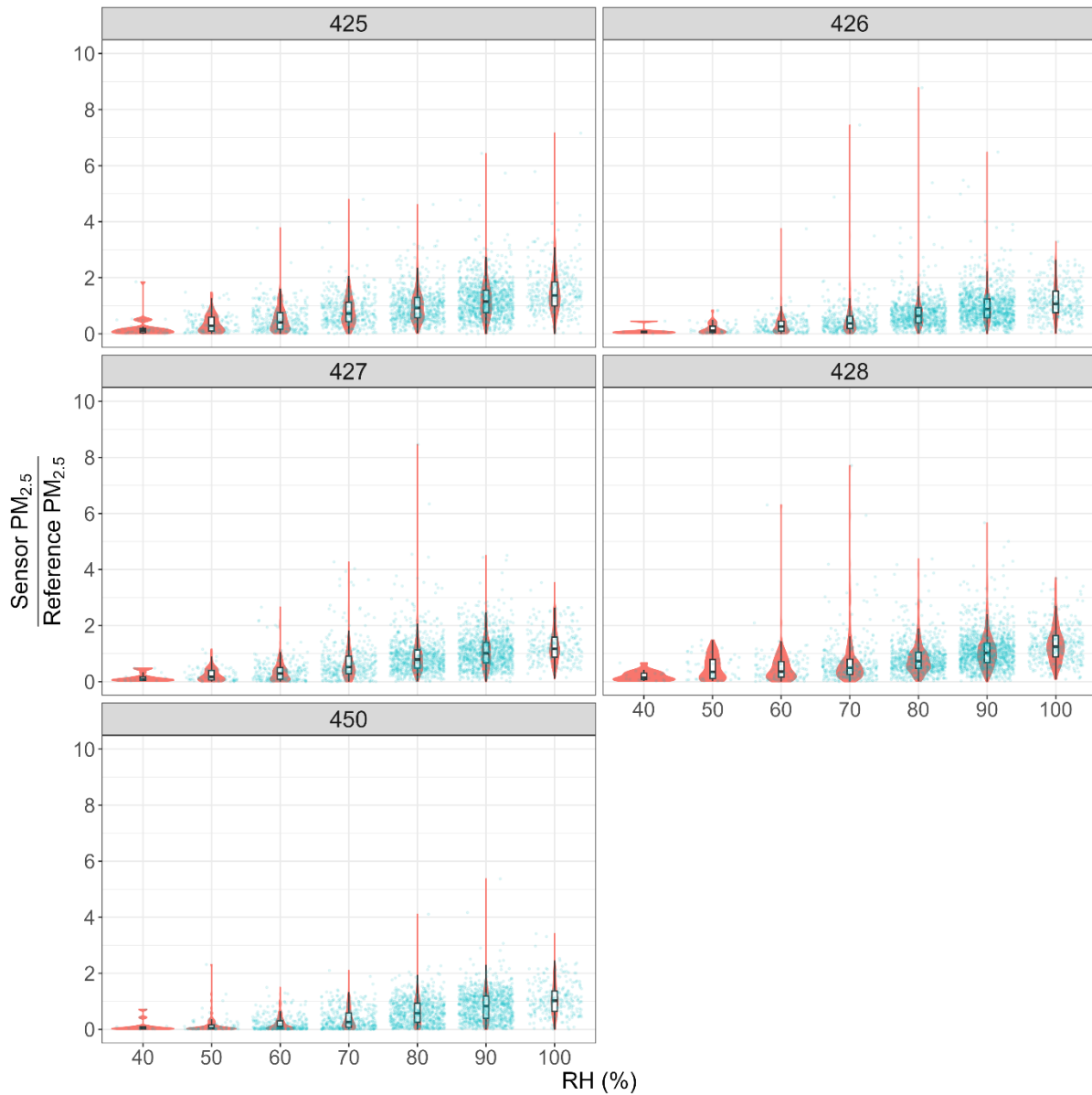


Figure 5: Violin boxplots of the $PM_{2.5}$ ratio between LCS and reference instrument in Tønsberg for different relative humidity cases. The ratio in the vertical axis is unitless and the horizontal axis is in units of %. The blue points represent the $PM_{2.5}$ ratios in each RH bin. The violin boxplot provides information about the summary statistics of a parameter (median and interquartile range) and describes the shape of the statistical distribution of the data using a kernel density function. A higher probability is given in the wider sections of the violin plot.

Figure 5 presents the $PM_{2.5}$ ratio between the air quality sensors and the reference instrument as a function of relative humidity (RH). The violin boxplots visually represent summary statistics (median and interquartile range) and the statistical distribution of the $PM_{2.5}$ Sensor/Reference ratio for various RH bins. The ratios are clustered around or below 1, indicating that increasing relative humidity only has a slight impact on $PM_{2.5}$ variations during less polluted hours.

On the other hand, Figure A2 displays the mean biases ($MBE = \frac{\sum_{i=1}^n (LCS PM_{2.5} - Reference PM_{2.5})}{n}$) and dispersion errors ($RMSE = \sqrt{\frac{\sum_{i=1}^n (LCS PM_{2.5} - Reference PM_{2.5})^2}{n}}$) for both the initial (raw) and the humidity-corrected $PM_{2.5}$ data against RH. Interestingly, the LCS humidity-corrected $PM_{2.5}$ data exhibit higher mean biases and dispersion errors compared to the initial LCS $PM_{2.5}$. This suggests that the humidity correction

method employed does not lead to improvements in sensor $\text{PM}_{2.5}$ data compared to the reference instrument.

In summary, given that during the 03:00 to 07:00 time window (Figure 4, Figure 5 and Figure A2), a) the measured $\text{PM}_{2.5}$ range is similar between the air quality sensors and the reference instrument, b) the regression slopes (gain) are relatively close to unity (ranging from 0.87 to 1.1) as shown in Figure 4, and c) relative humidity has only a marginal effect on $\text{PM}_{2.5}$, further correction of the initially measured $\text{PM}_{2.5}$ data is deemed necessary.

4.3 Distribution of $\text{PM}_{2.5}$ in Sandefjord using sensors

4.3.1 Hourly variation and sensor-to-sensor intercomparison

The air quality sensors measured $\text{PM}_{2.5}$ 1-hour averages. Figure 6 shows the temporal variation of $\text{PM}_{2.5}$ for the five sensors of the Sandefjord network during the whole operational period. These sensors display similar temporal fluctuations, with extreme $\text{PM}_{2.5}$ peaks associated with local anthropogenic contributions. Seasonal variations are evident, with $\text{PM}_{2.5}$ concentrations showing lower values in the summer and higher values in the winter. Upon visual inspection, sensor ID450 consistently recorded lower $\text{PM}_{2.5}$ compared to the other sensors. Table 3 presents summary statistics for the hourly $\text{PM}_{2.5}$. The median $\text{PM}_{2.5}$ was below $5 \mu\text{g m}^{-3}$. The average $\text{PM}_{2.5}$ concentration was approximately $6 \mu\text{g m}^{-3}$ for ID450, which is roughly $2 \mu\text{g m}^{-3}$ lower than the average concentrations recorded by the other sensors. The spatial distribution of the average $\text{PM}_{2.5}$ is also shown in Figure A3a.

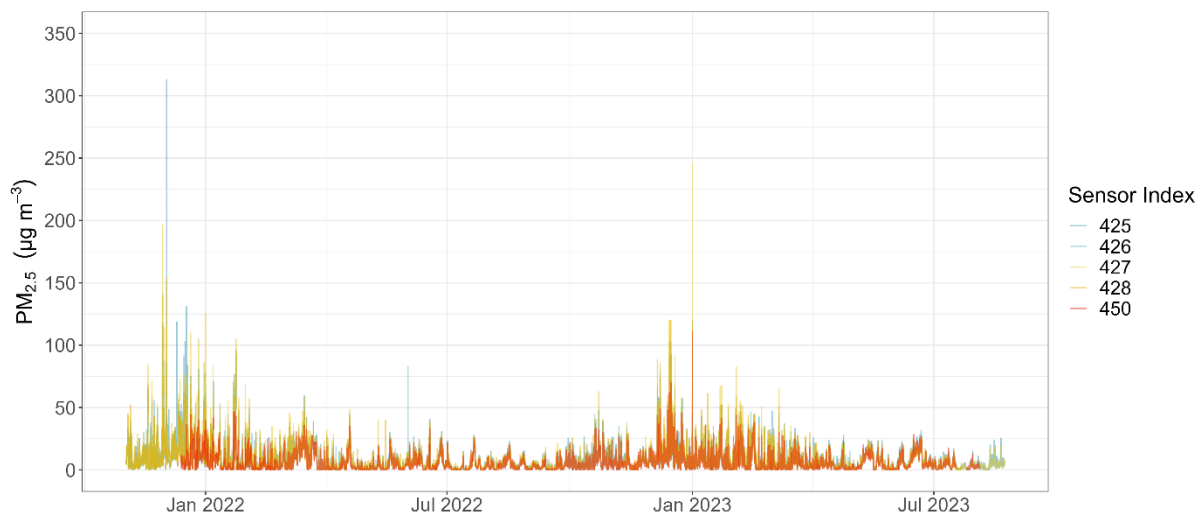


Figure 6: Hourly $\text{PM}_{2.5}$ time series for the Sandefjord air quality sensors. The vertical axis is in units of $\mu\text{g m}^{-3}$. Different colors correspond to sensors included in the air quality network.

Table 3: Descriptive statistics of hourly $PM_{2.5}$ concentrations for the air quality sensors. The statistical metrics are in units of $\mu g\ m^{-3}$. $Q_{25\%}$ and $Q_{75\%}$ are the 25% and 75% percentiles, and SD is the standard deviation of the hourly measurements.

Sensor Index	Min	$Q_{25\%}$	Median	Mean	SD	$Q_{75\%}$	Max
425	0	1.7	4.7	8	10.3	10.6	313
426	0	1.5	4	7	8.4	9.2	120.6
427	0	1.5	4.2	7.9	11.1	9.9	246.2
428	0	1.8	4.8	8	9.9	10.4	153.6
450	0	0.8	3	5.7	7.2	7.8	111

The hourly $PM_{2.5}$ exhibits significant variability, with standard deviations that surpass the average $PM_{2.5}$ values, as highlighted in Table 3 and shown Figure A3b. It is important to note that the extreme hourly $PM_{2.5}$, leading to peaks in Figure 6, are linked to specific events and are not consistently present throughout the air quality sensors' deployment period. The $Q_{75\%}$ metric, representing the 75th percentile of the data distribution, ranged from 7.8 to 10.6 $\mu g\ m^{-3}$, indicating that 75% of the hourly measurements fall below these values.

As depicted in Figure 6, there is a high level of correlation among all the sensors. Sensor-to-sensor intercomparison is a crucial method for assessing the sensors' performance by directly comparing their measurements, which, in turn, helps evaluate their reliability [7]. The sensor agreement is quantified by computing the average differences between the measurements when comparing sensor pairs. All sensors exhibit agreements within a range of -0.9 to $2.1\ \mu g\ m^{-3}$, suggesting that they are operating effectively. Notably, larger differences are observed in pairwise comparisons involving ID450.

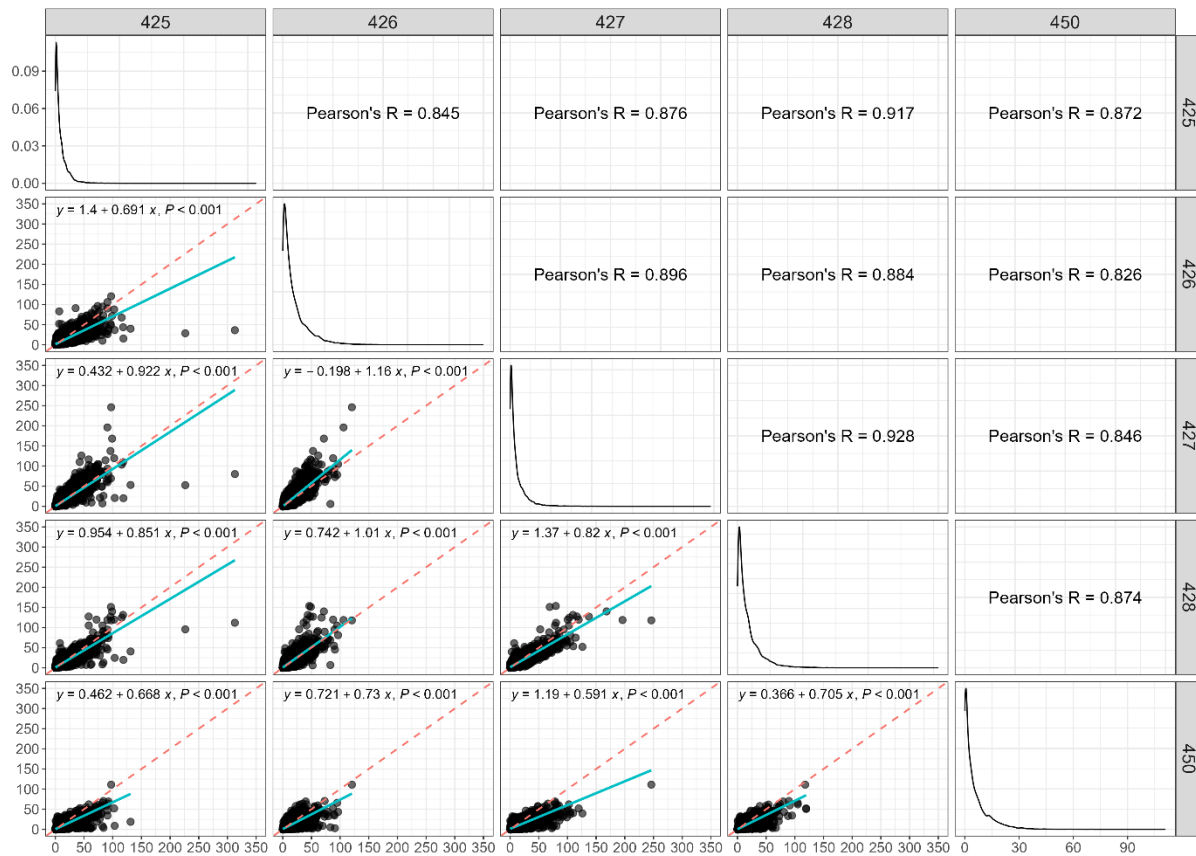


Figure 7: Sensor-to-sensor intercomparison of $PM_{2.5}$. Axes labels are in units of $\mu g m^{-3}$. The lower left panels show scatterplots of one sensor's output against the other, with the red dashed line indicating the 1:1 reference line. The equation inside the panels and blue solid line denote the linear regression fit to the data, where value P records the statistical significance of the linear model; if $P < 0.05$, the linear model is significant under the 95% confidence level. The diagonal panels show the $PM_{2.5}$ statistical density. The panels on the upper right show Pearson's R correlation coefficient.

The pairwise scatterplots in the lower panels of Figure 7 highlight the interrelationships between the $PM_{2.5}$ data from the different sensors. In all cases, these relationships are linear with Pearson's R correlation coefficients exceeding 0.8. However, when contrasting the sensors with ID450, it is evident that there are more noticeable deviations from the 1:1 reference line, with slopes ranging from 0.59 to 0.73, and the correlations in these specific comparisons become lower.

In the diagonal panels of Figure 7, the shapes of the $PM_{2.5}$ statistical densities are examined. These shapes are quite similar across all sensors, and they depict a skewed pattern that is particularly relevant to $PM_{2.5}$. Most values are below $10 \mu g m^{-3}$, emphasizing that most of the recorded $PM_{2.5}$ concentrations are in the lower range.

4.3.2 Daily and weekly variation

Hourly $PM_{2.5}$ time series data is typically aggregated into daily (24-hour) averages, which are of great significance, as they are related with national and World Health Organization (WHO) air quality limit and guideline values. A daily average is calculated assuming data completeness of 75% per day (more than 18 available hourly measurements). These daily averages provide valuable information about the overall air quality conditions in a specific area. However, it is important to note that examining hourly

PM_{2.5} time series data can offer valuable insights, including the identification of air pollution hot spots, pinpoint areas and times with high PM_{2.5} concentrations, and recognize specific factors contributing to the observed PM_{2.5} variability throughout the day. The daily PM_{2.5} time series of Figure 8 reveal a consistent day-to-day variation across all sensors. These patterns exhibit peaks at the same timestamps. Any variations in the peaks can be attributed to differences in the intensity and location of local sources.

Upon closer examination, it is noteworthy that among the four sensors mentioned (ID425, ID426, ID427, ID428) situated in Sandefjord's urban area, ID426 consistently records lower PM_{2.5} concentrations in comparison to the other sensors placed near the port area. This difference underscores the localized nature of PM_{2.5} pollution, with the sensors closer to the port area exhibiting higher concentrations, likely due to traffic and maritime activities in their vicinity.

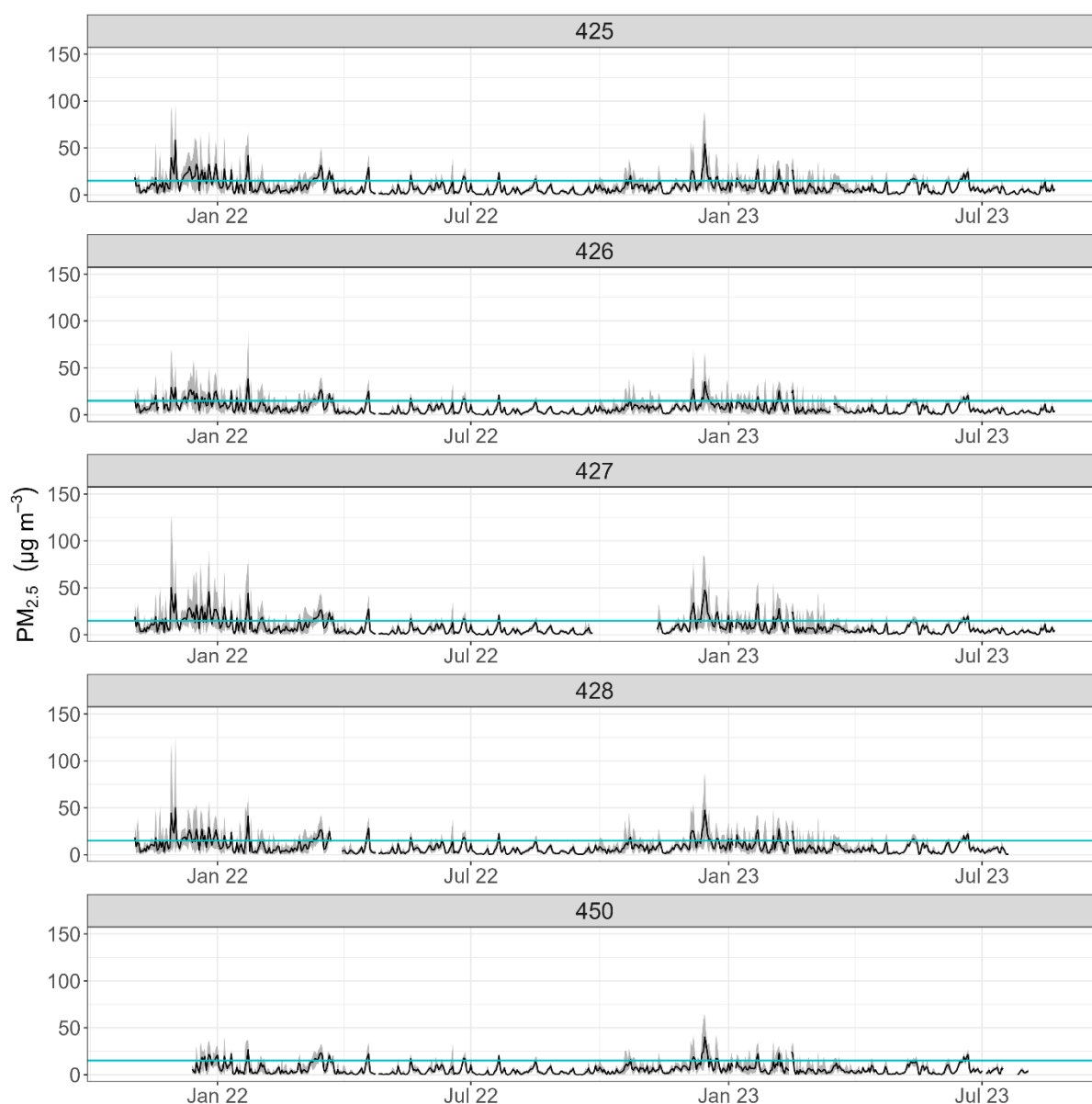


Figure 8: Daily $PM_{2.5}$ time series for the Sandefjord air quality sensors. The vertical axis is in units of $\mu g m^{-3}$. The black line is for the daily (24-h averaged) $PM_{2.5}$ concentrations. The shaded area corresponds to the difference between the 90% and 10% percentiles, $Q_{90\%} - Q_{10\%}$, with $Q_{X\%}$ the $X\%$ percentile of the data. The blue horizontal line defines the national $PM_{2.5}$ limit value ($15 \mu g m^{-3}$).

Table 4: Descriptive statistics of daily (24-h average) $PM_{2.5}$ concentrations for the air quality sensors. The statistical metrics are in units of $\mu g\ m^{-3}$. $Q_{25\%}$ and $Q_{75\%}$ are the 25% and 75% percentiles, and SD is the standard deviation of the daily data.

Sensor Index	Min	$Q_{25\%}$	Median	Mean	SD	$Q_{75\%}$	Max
425	0.1	3.0	5.9	8.1	7.4	11.1	58.3
426	0.1	2.5	5.3	7.0	6.0	9.9	38.2
427	0.3	2.6	5.4	7.9	7.8	10.6	50.3
428	0.1	3.0	6.0	8.0	6.9	10.8	49.9
450	0	1.6	3.9	5.7	5.6	7.8	40.3

Table 4 provides descriptive statistics for the daily $PM_{2.5}$ in $\mu g m^{-3}$. The long-term daily average $PM_{2.5}$ is consistent for all urban sensors, except for ID450. Daily $PM_{2.5}$ concentrations, in general, remain below both the national limit value and WHO guidelines, set at $15 \mu g m^{-3}$ (as indicated by the blue horizontal line in Figure 8). $PM_{2.5}$ concentrations above this level are primarily observed during the winter months.

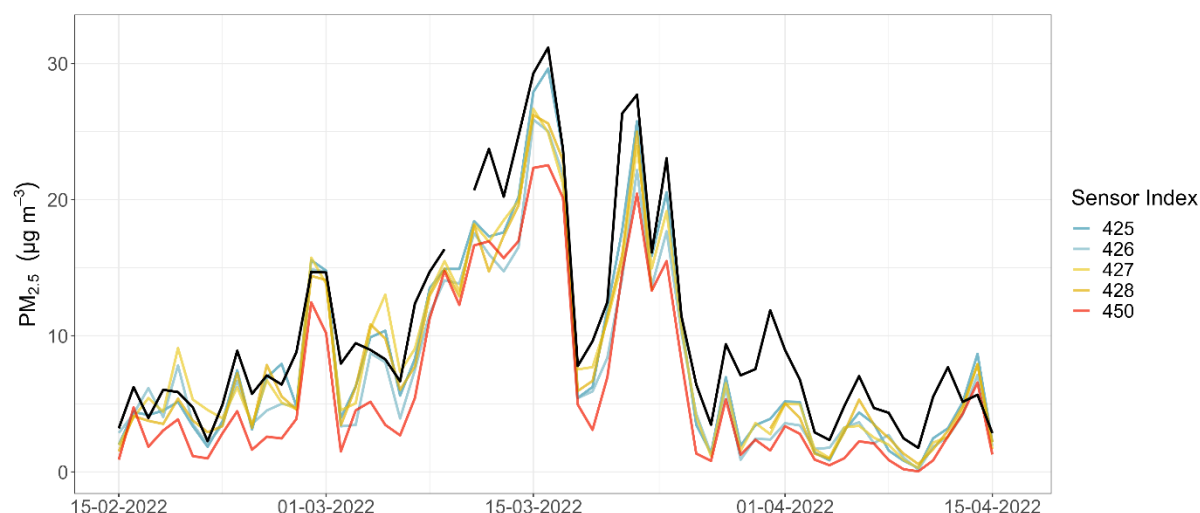


Figure 9: Time series of daily $PM_{2.5}$ for the Sandefjord air quality network sensors and the reference site in Tønsberg (black line) from 15-02-2022 to 15-04-2022. This period is selected to show the $PM_{2.5}$ variations for the PM episode observed in March 2022. The vertical axis is in units of $\mu g m^{-3}$.

It is interesting to discuss the daily $PM_{2.5}$ of the reference site in Tønsberg and the air quality sensors for the long-range PM episode in March 2022 (Figure 9). In March 2022, $PM_{2.5}$ showed strongly variable concentrations throughout the month. The PM episode affected whole Europe, and it was characterized as complex and dynamic, involving contributions from residential heating, traffic emissions, wildfires and North African desert dust intrusions ([8],[9]). Both the low-cost sensors and the reference site measure high $PM_{2.5}$ with the LCS to provide lower concentrations. The air quality sensors replicate to a large degree the intensity and duration of the PM episode, generally exhibiting a temporal pattern similar to that of the reference site in Tønsberg.

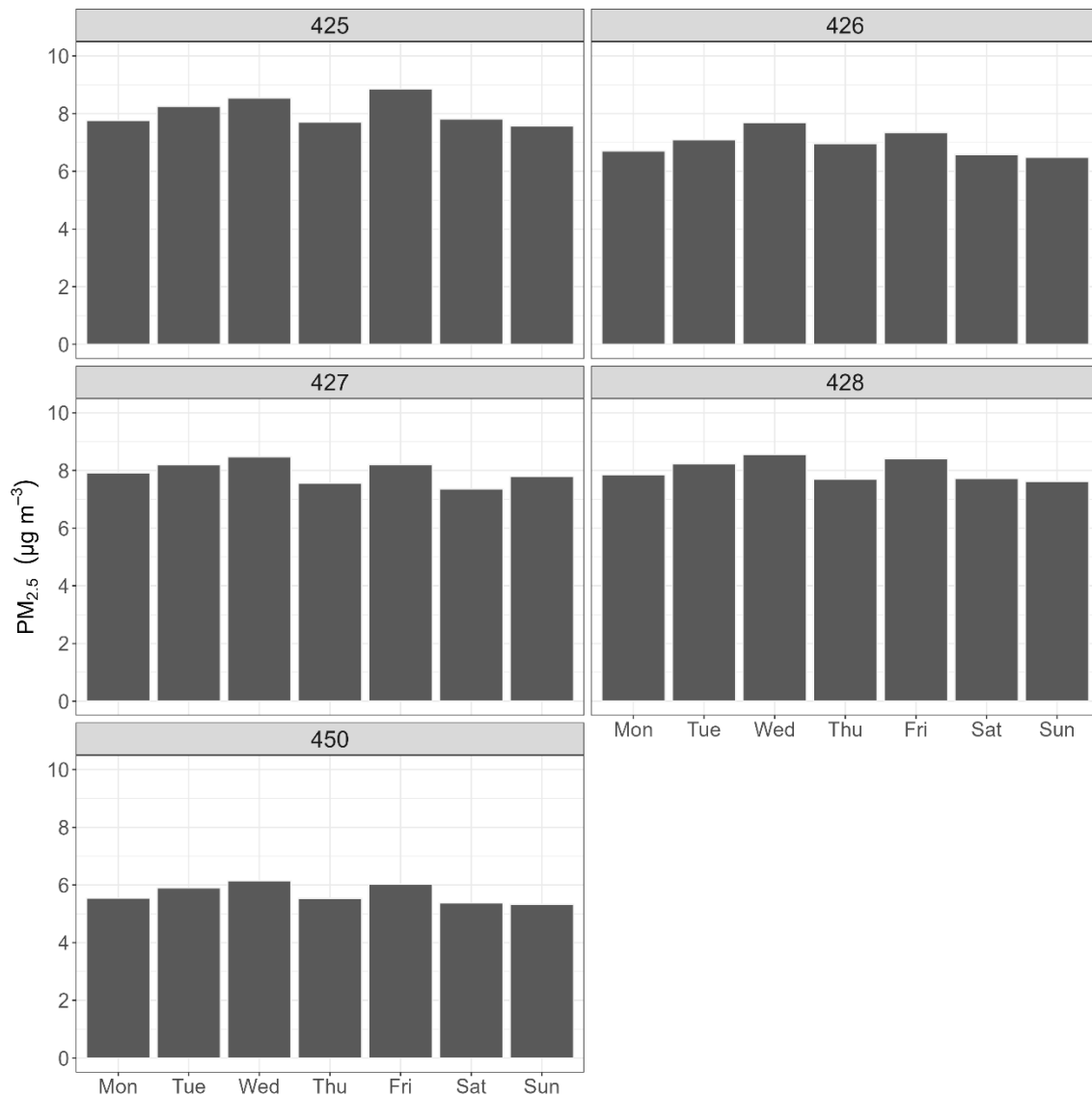


Figure 10: Weekly distribution of PM_{2.5} for the Sandefjord air quality network sensors. The vertical axis is in units of µg m⁻³. The labels in the horizontal axis are Mon – Monday, Tue – Tuesday, Wed – Wednesday, Thu – Thursday, Fri – Friday, Sat – Saturday and Sun – Sunday.

In Figure 10, the daily PM_{2.5} data is aggregated and averaged for each day of the week, separately for each sensor. All sensors exhibit a similar pattern, with no significant changes in PM_{2.5} levels observed across different days of the week.

Similar concentrations across different days of the week are common in many urban areas. Certain sources of PM_{2.5} pollution, such as traffic and other emissions, may operate consistently throughout the week, contributing to this stability. It is also noteworthy that differences in PM_{2.5} concentration may be observed between weekdays and weekends, due to the decrease in work-related activities and the reduction of vehicular traffic emissions. However, comparing the two periods, marginal differences in PM_{2.5} can be recorded according to Figure 10.

4.3.3 Monthly and seasonal variation

Monthly average PM_{2.5} data is visually represented in both Figure 11 and Figure A4. These figures provide insights into the variations in PM_{2.5} levels, showcasing specific concentration ranges for

different sensor IDs. Only months including more than 75% of daily values are considered as valid. ID425, ID426, ID427, ID428, and ID450 have varying $PM_{2.5}$, with respective ranges of $3.5 - 21.3 \mu g m^{-3}$, $2.8 - 16.6 \mu g m^{-3}$, $2.6 - 21.5 \mu g m^{-3}$, $3.3 - 18.6 \mu g m^{-3}$, and $2.4 - 12.7 \mu g m^{-3}$, respectively.

All sensors exhibit a distinct seasonal pattern, with the highest monthly averages in December for both 2021 and 2022. Notably, ID450 consistently records considerably lower monthly concentrations than the other sensors, resulting in monthly deviations ranging from -0.2 to $9.8 \mu g m^{-3}$.

Comparing the air quality sensors within the Sandefjord area reveals a notable disparity. $PM_{2.5}$ in close proximity to the port area consistently exceed the concentrations observed in ID426 (as depicted in Figure 1). These disparities in monthly $PM_{2.5}$ values range from -0.3 to $5 \mu g m^{-3}$, with an average difference of approximately $1 \mu g m^{-3}$, emphasizing the significance of location in air quality measurements within the region.

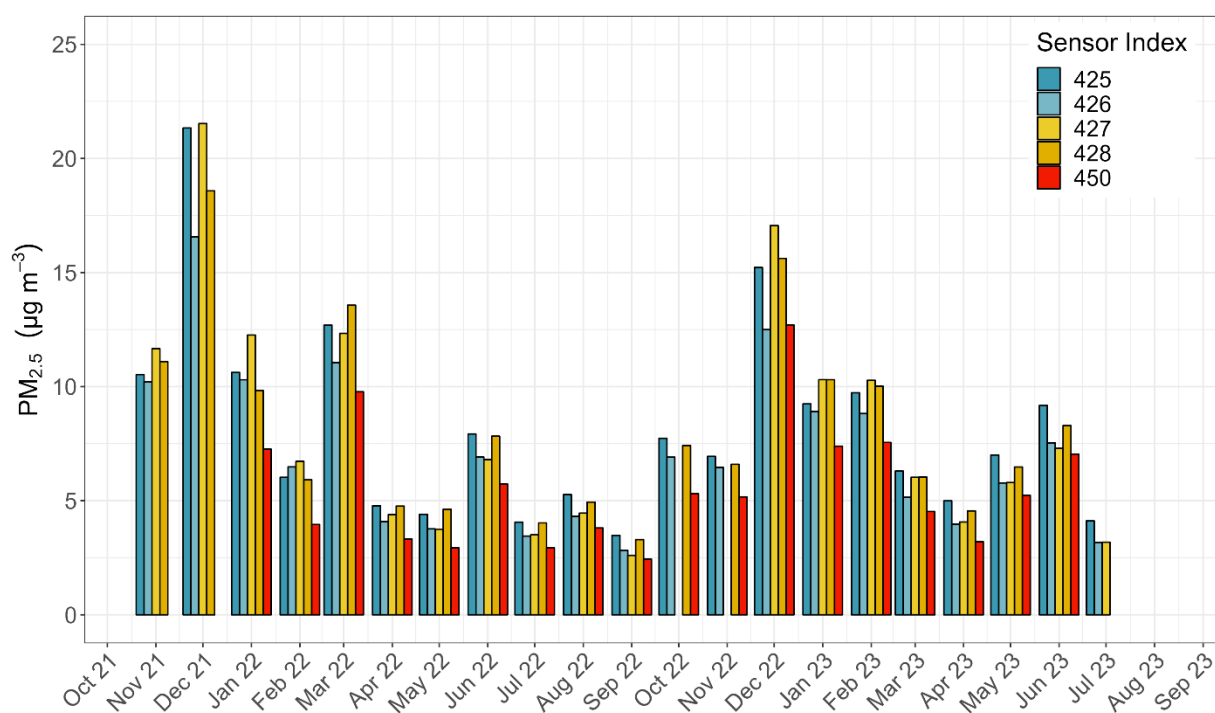


Figure 11: Bar plots of monthly averaged $PM_{2.5}$ measured by the five sensors. The vertical axis is in units of $\mu g m^{-3}$. Different colors correspond to sensors included in the Sandefjord air quality network.

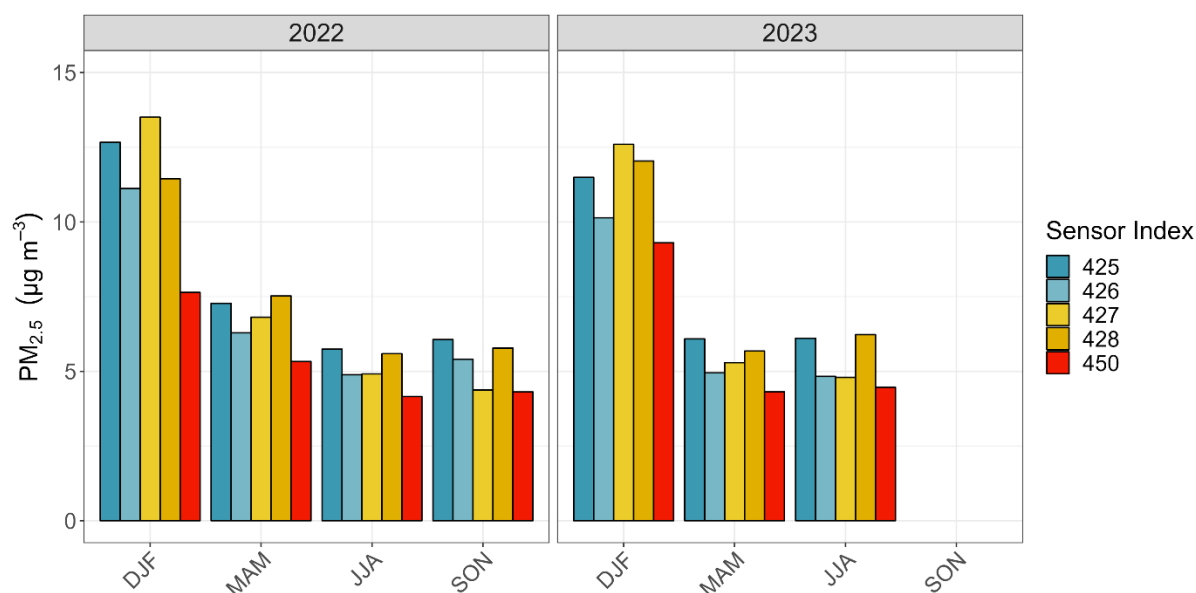


Figure 12: Bar plots of seasonally averaged $PM_{2.5}$. The vertical axis is in units of $\mu g m^{-3}$. Different colors correspond to sensors included in the Sandefjord air quality network. The labels in the horizontal axis are for different seasons with DJF – Winter (December, January, February), MAM – Spring (March, April, May), JJA – Summer (June, July, August) and SON – Autumn (September, October, November).

Elevated local emissions, coupled with reduced atmospheric mixing, can be attributed to the elevated concentrations of $PM_{2.5}$ during colder periods. Figure 12 provides the seasonal averages for each year and sensor. Winter stands out as a season with significantly elevated $PM_{2.5}$ concentrations, nearly double those observed during other seasons. Across all sensor locations, except ID450, $PM_{2.5}$ consistently remains above $10 \mu g m^{-3}$ during winter. When assessing the seasonal differences in $PM_{2.5}$ between 2022 and 2023, it is noteworthy that $PM_{2.5}$ levels in 2022 are slightly higher during the winter and spring periods when compared to 2023.

4.3.4 Yearly variation

The annual averages are calculated for each sensor, assuming a data completeness of 75%. Generally, if the data coverage falls below 75% for the annual averaging period, annual statistics should not be employed for air quality assessments. Figure 13 illustrates the $PM_{2.5}$ annual averages of 2022 for the Sandefjord sensors. The year 2022 is deemed complete for all sensors and the number of days ranges between 319 and 364. Therefore, the results for 2022 are discussed here.

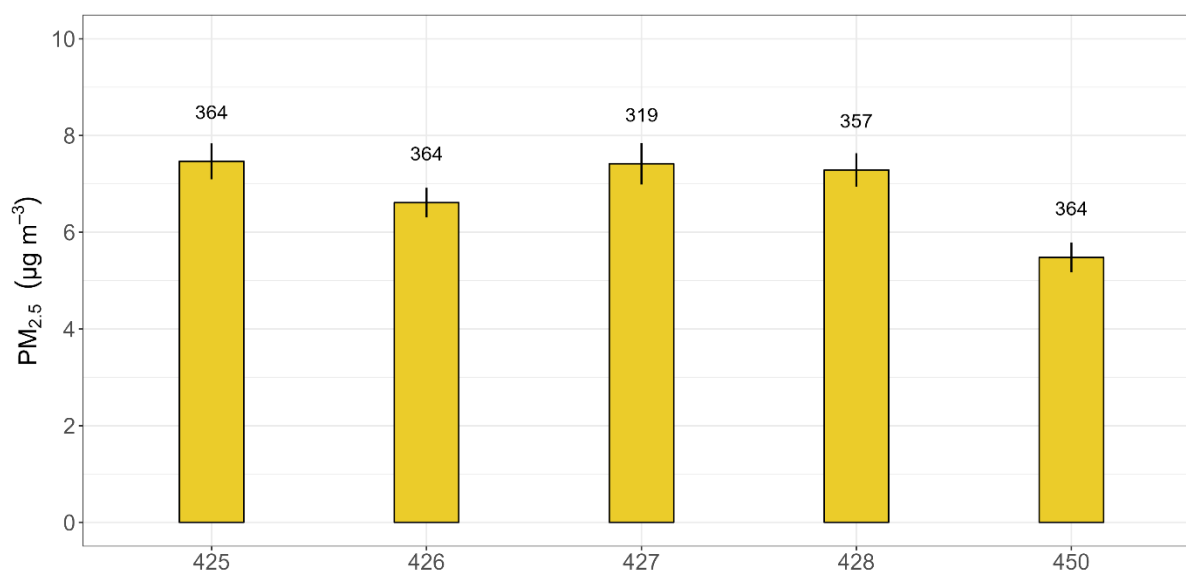


Figure 13: Bar plots of 2022 annual average PM_{2.5}. The vertical axis is in units of µg m⁻³. The number above each bar corresponds to the number of days included in the calculation of annual average. The vertical lines in each bar correspond to the standard error of the mean.

The annual concentrations (\pm standard error of the mean) of PM_{2.5} for 2022, recorded by various sensors, are as follows: 7.5 ± 0.4 µg m⁻³ (ID425), 6.6 ± 0.3 µg m⁻³ (ID426), 7.4 ± 0.4 µg m⁻³ (ID427), 7.3 ± 0.3 µg m⁻³ (ID428), and 5.5 ± 0.3 µg m⁻³ (ID450). The standard error of the mean is calculated by $SE = s/\sqrt{N}$ with s the standard deviation and N the number of available days in a calendar year. For air pollution regulatory purposes, the limit value for PM_{2.5} over a calendar year is 10 µg m⁻³ (Table 1). To determine if a limit value is exceeded, measurements spanning an entire (complete) calendar year are necessary. The year 2022 has a data completeness exceeding 75% whereas 2023 has a data coverage ranging from 55% to 64% across various sensors. In 2021, sensor data are available only for two months (November and December). Consequently, they cannot be compared to the limit values due to incomplete data coverage. It is noteworthy that all air quality sensors in Sandefjord area report values below 10 µg m⁻³ for 2022. On the other hand, the assessment thresholds for PM_{2.5} regarding human health over a calendar year are 5 µg m⁻³ (lower assessment threshold) and 7 µg m⁻³ (upper assessment threshold)⁴. The annual PM_{2.5} values for 2022 are either comparable to or lower than the upper assessment threshold. It is important to highlight that sensors are not reference equivalent and that therefore the levels above can only be read as indicative measurements. Therefore, the results above the upper assessment threshold should be understood that although the current limit value of 10 µg m⁻³ is not exceeded, there is a possibility that the more stringent annual limit value of 5 µg m⁻³ (Table 1) will be exceeded.

4.3.5 Diurnal variation

The diurnal pattern of PM_{2.5} in urban settings displays a distinctive pattern varying throughout the day. This pattern is shaped by a range of factors, encompassing human activities, meteorological conditions and atmospheric processes. Typically, within urban areas, PM_{2.5} rises during the early morning, especially during rush hour, primarily due to increased vehicular emissions into a still shallow boundary layer and the resuspension of particles from roads. From mid-morning to early afternoon, when traffic is lower and atmospheric mixing is improved, PM_{2.5} concentrations tend to decrease. However, this

⁴ <https://lovdata.no/dokument/LTI/forskrift/2022-06-23-1189>

reduction might not be substantial as local and natural sources can affect $PM_{2.5}$ levels. In the evening, $PM_{2.5}$ increases again due to rush hour traffic and less vertical mixture. During the evening, in winter, contributions from residential heating become more prominent, leading to a further rise in $PM_{2.5}$ levels. As temperatures drop in the evening, stable atmospheric conditions become more prevalent, trapping atmospheric pollutants near the surface. It is worth noting that the diurnal $PM_{2.5}$ pattern varies across urban areas due to differences in geography, topography climate, urban development, local emissions, and regulatory measures.

Examining the intraday variability of $PM_{2.5}$ in Sandefjord offers valuable insights into the predominant sources influencing this specific area's air quality. The average diurnal $PM_{2.5}$ profile for the entire operational of the sensors' network period is visually depicted in Figure 14 and Figure A5, revealing a distinctive bimodal pattern. $PM_{2.5}$ exhibits two distinct peaks, one in the morning and another in the evening, which are closely tied to different local emissions. The diurnal $PM_{2.5}$ pattern for ID450 consistently records lower values than those observed at the other sensor locations, with differences during evening exceeding $4 \mu g m^{-3}$. This discrepancy underscores the differences in the extent of local emission sources. Since the anthropogenic emissions vary throughout the year, with factors like residential heating being more prevalent in the winter, the diurnal profiles vary across different calendar seasons (Figure 16).

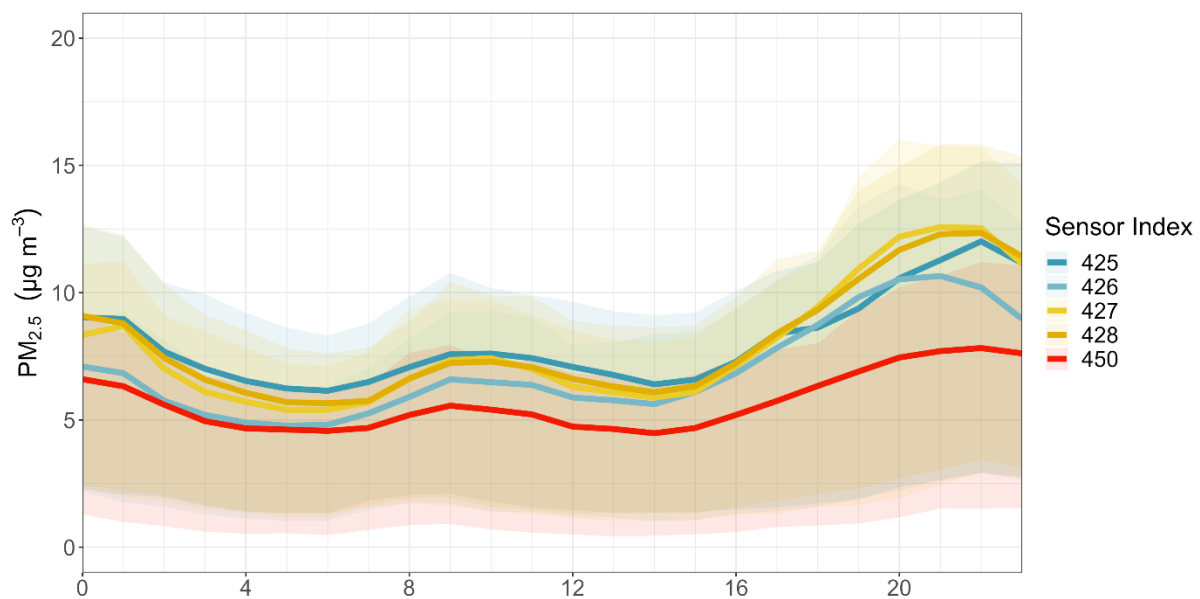


Figure 14: Diurnal variation of $PM_{2.5}$ for the Sandefjord air quality sensors. The vertical axis is in units of $\mu g m^{-3}$. The colored lines are the average $PM_{2.5}$ for the different sensors. The shaded area corresponds to the interquartile range, $IQR = Q_{75\%} - Q_{25\%}$, with $Q_{X\%}$ the $X\%$ percentile of the data.

The diurnal variation of $PM_{2.5}$ for each season, obtained by averaging daily profiles for each season, is represented in Figure 15. Additionally, Figure A6, Figure A7, Figure A8 and Figure A9 illustrate the spatial distribution of $PM_{2.5}$ in each season and each hour of the day. During the summer season, $PM_{2.5}$ exhibits a relatively flat pattern, suggesting a minimal impact from local sources. The concentration ranges for this period are $4.5 - 7.2 \mu g m^{-3}$ (ID425), $4.1 - 5.8 \mu g m^{-3}$ (ID426), $3.8 - 6.2 \mu g m^{-3}$ (ID427), $4.9 - 7.2 \mu g m^{-3}$ (ID428), and $3.6 - 6.1 \mu g m^{-3}$ (ID450), indicating minor variation around their average values and overall favorable air quality conditions.

Conversely, the diurnal profile for other seasons shows a bimodal pattern, characterized by morning peaks (between 08:00 and 09:00) and evening peaks (between 19:00 and 21:00). This bimodality is particularly prominent during winter. In spring and autumn, the morning peak exhibits comparatively modest values, slightly exceeding the daily $\text{PM}_{2.5}$ average. The diurnal amplitude, the difference between the maximum and minimum $\text{PM}_{2.5}$ throughout the day, during winter is substantial, recording $14.2 \mu\text{g m}^{-3}$ (ID425), $14.8 \mu\text{g m}^{-3}$ (ID426), $18.7 \mu\text{g m}^{-3}$ (ID427), $15.1 \mu\text{g m}^{-3}$ (ID428), and $9.6 \mu\text{g m}^{-3}$ (ID450). In the transitional seasons of spring (MAM) and autumn (SON), the diurnal amplitude is lower compared to winter, with $\text{PM}_{2.5}$ ranges spanning from 3.2 to $6 \mu\text{g m}^{-3}$ and 3.9 to $10.8 \mu\text{g m}^{-3}$, respectively.

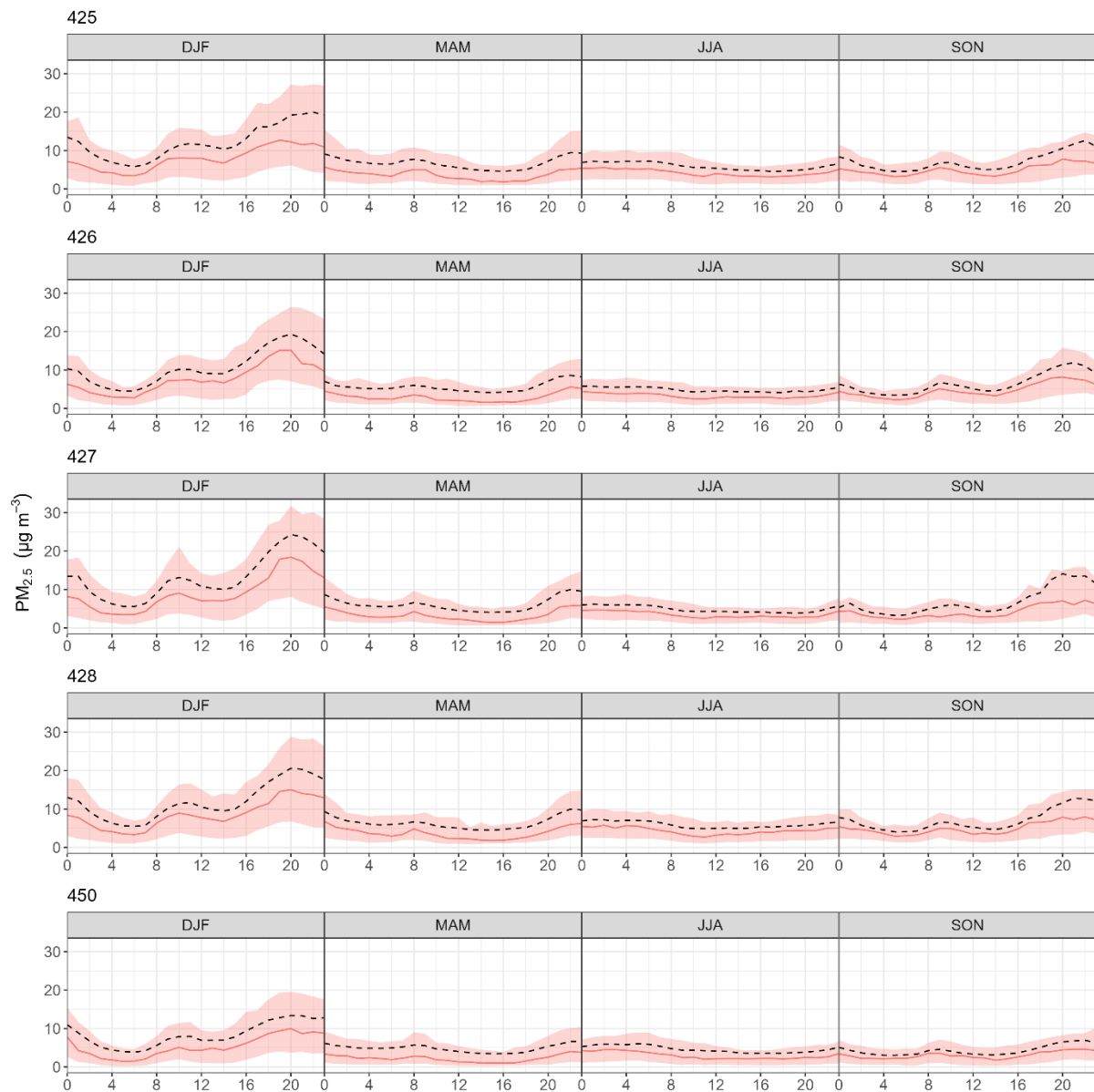


Figure 15: Diurnal distribution of $PM_{2.5}$ for each season and sensor included in the Sandefjord air quality network. The vertical axis is in units of $\mu\text{g m}^{-3}$. The red and black lines are the median and the average $PM_{2.5}$, respectively. The shaded area corresponds to the interquartile range, $IQR = Q_{75\%} - Q_{25\%}$, with $Q_{X\%}$ the $X\%$ percentile of the data. The header in each panel represents the season with DJF – Winter (December, January, February), MAM – Spring (March, April, May), JJA – Summer (June, July, August) and SON – Autumn (September, October, November).

Examining the peak characteristics within diurnal profiles also offers valuable insights into the magnitude and potential of the predominant sources. Notably, vehicular emissions are the primary drivers behind the morning peak. To quantify the magnitude of morning emissions using the diurnal $PM_{2.5}$ distribution, the difference between the morning peak $PM_{2.5}$ and the minimum $PM_{2.5}$ is considered, denoted as $\Delta PM_{2.5, \text{morning peak}}$ ($\Delta PM_{2.5, \text{morning peak}} = PM_{2.5, \text{morning peak}} - \min(PM_{2.5})$). The minimum $PM_{2.5}$ from the diurnal profile serves as the lower threshold, signifying that any $PM_{2.5}$

below this limit is entirely attributed to regional sources. $\Delta PM_{2.5, \text{ morning peak}}$ ranges from 4.2 to 7.6 $\mu\text{g m}^{-3}$.

The evening peak is shaped by a combination of factors, including residential heating activities and continued traffic, as well as reduced atmospheric mixing with this pattern being more pronounced during the winter months. To examine the extent of $PM_{2.5}$ increase in the evening, the difference in $PM_{2.5}$ between the evening and morning peaks, ($\Delta PM_{2.5, \text{ evening peak}} = PM_{2.5, \text{ evening peak}} - PM_{2.5, \text{ morning peak}}$) is computed. In this analysis, the lower threshold is $\Delta PM_{2.5, \text{ morning peak}}$, assuming that $PM_{2.5}$ does not experience a significant reduction after reaching the first maximum. Any addition in $PM_{2.5}$ is attributed to contributions from distinct emission sources, such as residential heating which is more pronounced during evening hours. Furthermore, the boundary layer height is lower during nighttime, indicating that the emissions are added/discharged into a smaller air volume than in the middle of the day. For instance, $\Delta PM_{2.5, \text{ evening peak}}$ ranges from 8.2 $\mu\text{g m}^{-3}$ (ID425), 9.1 $\mu\text{g m}^{-3}$ (ID426), 11.1 $\mu\text{g m}^{-3}$ (ID427), 8.9 $\mu\text{g m}^{-3}$ (ID428), and 5.4 $\mu\text{g m}^{-3}$ (ID450).

A similar approach can be applied in spring and autumn seasons. In autumn, where at least the evening peak is discernible, $PM_{2.5}$ experiences a difference of less than $\sim 3 \mu\text{g m}^{-3}$ compared to the diurnal minimum $PM_{2.5}$. The discrepancy between evening and morning peaks extends from 2.3 $\mu\text{g m}^{-3}$ (ID450) to 8 $\mu\text{g m}^{-3}$ (ID427).

4.3.6 $PM_{2.5}$ vs. air temperature – a proxy for residential heating

$PM_{2.5}$ expresses a complex relationship with air temperature, especially when residential heating is dominating. This relationship is more pronounced in cases where residential heating relies on wood combustion. Low temperature intensifies heating demand implying the extensive contribution from residential heating emissions on the observed $PM_{2.5}$ concentrations. The relationship between $PM_{2.5}$ and air temperature is also modulated by the concurrent meteorological conditions. More specifically, a combination of low wind speeds, cloudless skies during night and low temperatures at the ground level leads to inversion conditions, limiting vertical mixing and atmospheric dispersion processes. Under these circumstances, $PM_{2.5}$ stays at high levels. In Nordic countries, residential wood burning stands as one of the most significant local contributors to air pollution, accounting for a substantial portion of house heating $PM_{2.5}$, estimated at 50-80% ([10],[11]). When residential wood burning coincides with specific meteorological conditions, it results in high $PM_{2.5}$ levels, particularly during the cold months.

As depicted in Figure 15, the diurnal $PM_{2.5}$ variation among air quality sensors reveals increased values in the evening, primarily attributed to local anthropogenic activities and residential heating demand. The heat maps presented in Figure 16 provide a comprehensive visualization of $PM_{2.5}$ concentrations on both a daily and monthly basis, enabling the identification of periods with elevated concentrations. A similar pattern emerges across all sensors, characterized by rising $PM_{2.5}$ from November to March, particularly in the time window from 15:00 to 23:00. As previously discussed, the evening peak in $PM_{2.5}$ concentrations is primarily driven by vehicular traffic and residential heating emissions, while high $PM_{2.5}$ persists during the colder months and extended night hours.

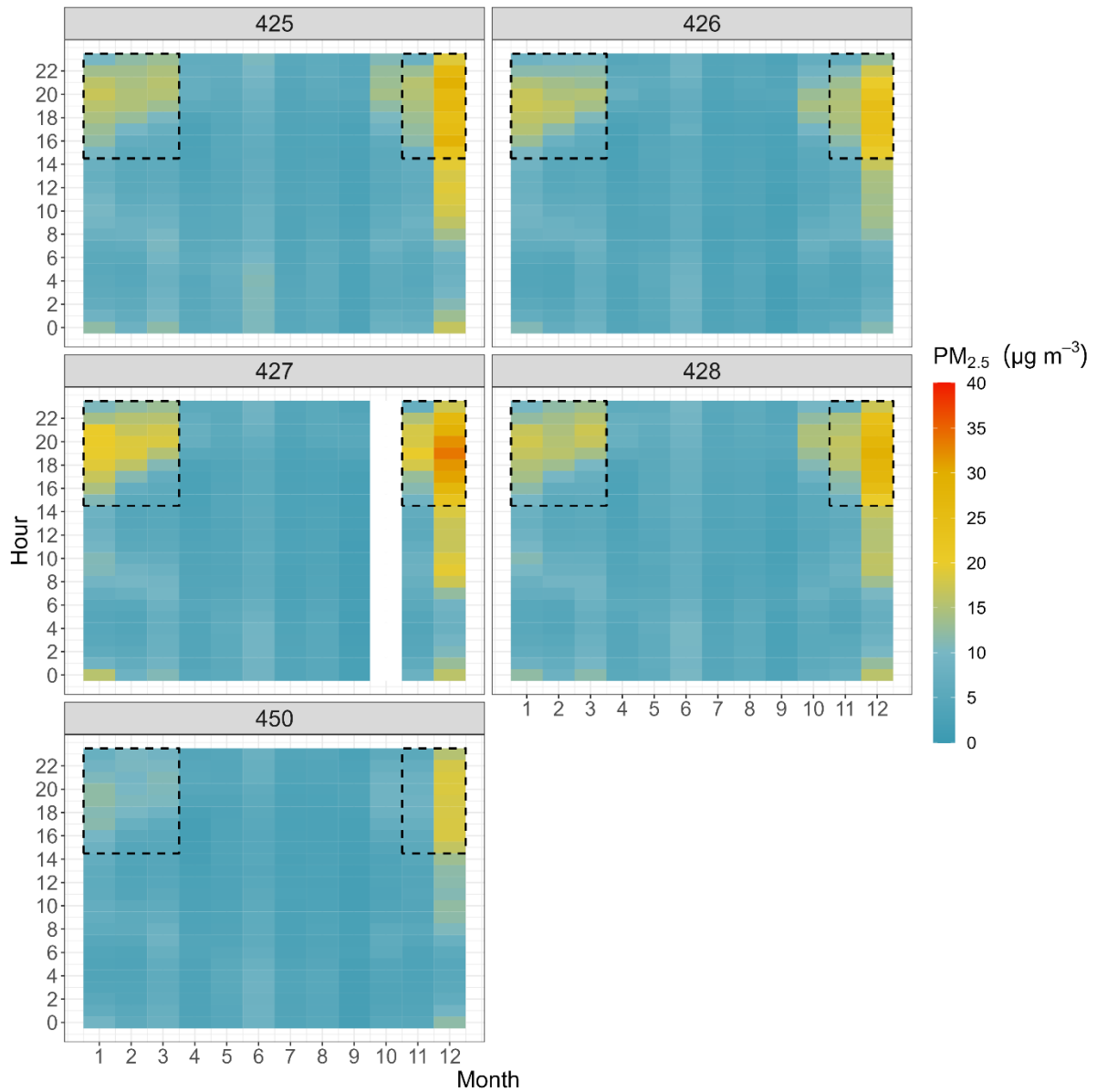


Figure 16: Heatmaps of PM_{2.5} by month and hour of the day for each LCS. The colored regions are in units of $\mu\text{g m}^{-3}$ with warm colors for high concentrations. The black dashed rectangles (horizontal axis: 11 (November) – 3 (March), vertical axis: 15:00 – 23:00) represent the areas with persistently high PM_{2.5}.

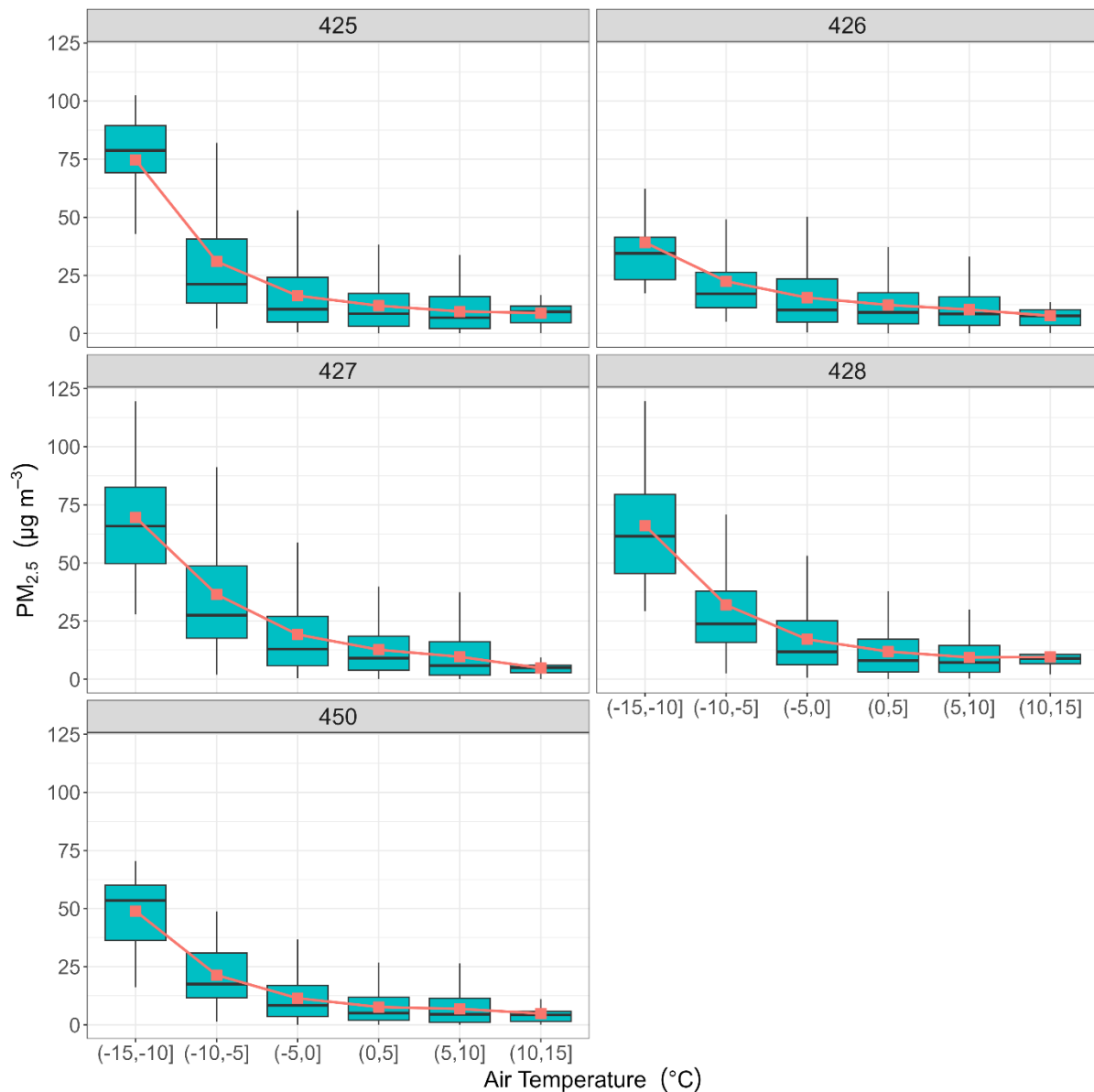


Figure 17: Boxplots of $PM_{2.5}$ against air temperature using hourly data from November to March and from 15:00 to 23:00. The horizontal and vertical axes labels are in $^{\circ}C$ and $\mu g m^{-3}$ units, respectively. Air temperature bins are created using a bin width of $5^{\circ}C$. The horizontal black line and the red point inside the whiskers denote the median and the average values of the measurements included in each bin.

Figure 17 offers an overview of the linkage between $PM_{2.5}$ and air temperature, utilizing data obtained from November to March during the hours of 15:00 to 23:00. The relationship between $PM_{2.5}$ and air temperature exhibits a non-linear pattern, showing a decreasing tendency of $PM_{2.5}$ as air temperature increases. $PM_{2.5}$ is significantly correlated to temperature, with correlation coefficients ranging from -0.46 (ID450) to -0.28 (ID426). The increase in $PM_{2.5}$ is particularly pronounced when air temperatures drop below $0^{\circ}C$. This correlation mainly reflects the impact of residential heating activities on $PM_{2.5}$ concentrations, becoming more evident in low-temperature conditions where the stability conditions of the atmosphere also play a significant role.

5 Local and regional sources

Air quality in urban environments is influenced by a combination of regional and local sources. Several works employed various methodologies to distinguish these emission sources, typically through:

- a) Statistical Techniques such as Gaussian mixture models, spectrum analysis, and time series analysis ([12],[13],[14]).
- b) Comparisons with background sites that are less affected by local contributions and can be used as reference points for assessing the impact of local sources [15].
- c) Analysis of diurnal profiles: analyzing the diurnal patterns of air pollutants over extended periods, such as a month or a season, could extract useful insights about the local and regional contributions ([15],[16]).

To determine the regional (background) and local contributions to air pollution, the analysis of the diurnal $PM_{2.5}$ profile was performed on a monthly basis. This involved averaging the diurnal distributions of $PM_{2.5}$ over a month-long period. Subsequently, the minimum $PM_{2.5}$ value within the monthly diurnal profile is considered the average regional concentration. This is an overestimation of the regional contribution since it is assumed that the minimum $PM_{2.5}$ is entirely regional. The local concentration is then calculated by subtracting this regional concentration from the monthly $PM_{2.5}$, allowing for a distinction between regional and local sources of air pollution.

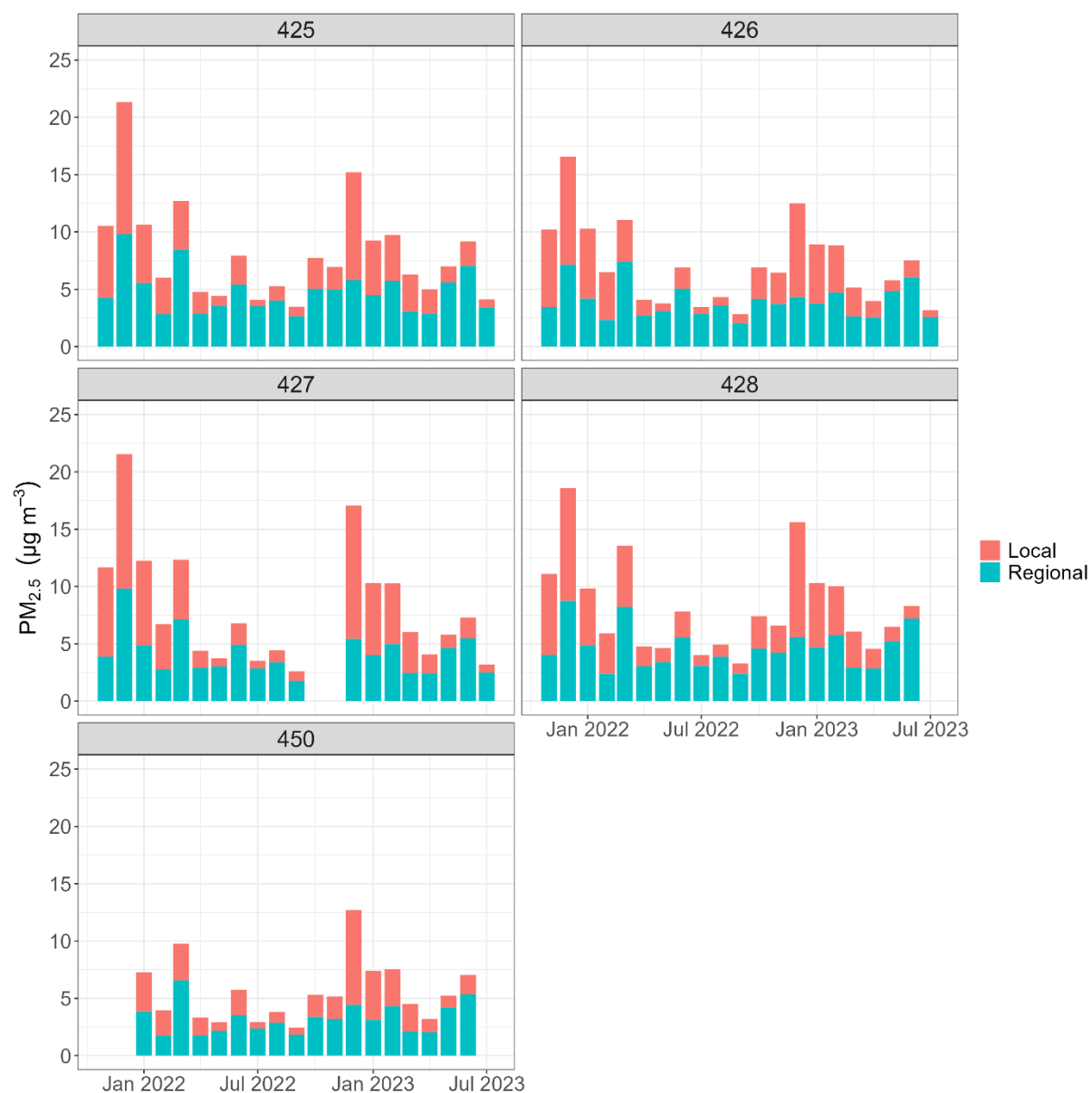


Figure 18: Time series of the average local and regional $PM_{2.5}$ calculated by analyzing the monthly diurnal profiles. The vertical axis is in units of $\mu g m^{-3}$.

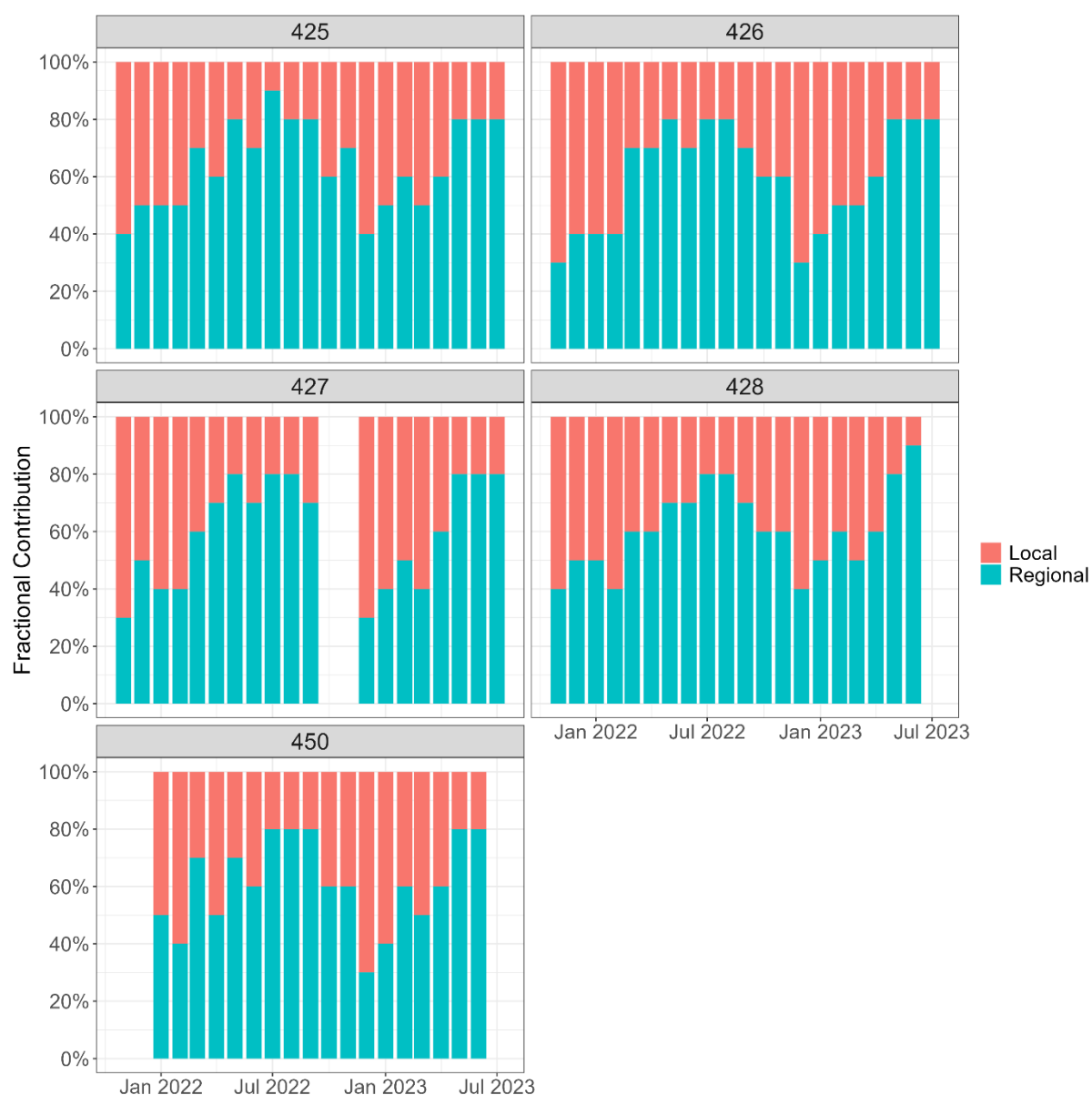


Figure 19: Fractional contribution of average local and regional $PM_{2.5}$.

Figure 18 and Figure 19 provide an insightful representation of the local and regional average $PM_{2.5}$ concentrations and their respective contributions to the overall average monthly $PM_{2.5}$ levels. The key findings can be derived from the figures above as follows:

- Regional contribution:** $PM_{2.5}$ from regional sources exhibits fluctuations, with an average of approximately $4 \mu g m^{-3}$. Depending on the sensor site, the variability can be as much as $1 \mu g m^{-3}$. On average, regional sources account for roughly 60% of the total $PM_{2.5}$. Notably, in March 2022, the regional contribution surpasses 60%. This observation signifies the effectiveness of diurnal profile analysis in discerning non-local PM influences, subsequently adjusting the regional $PM_{2.5}$ levels to account for this specific effect.
- Local Contribution:** The contribution from local sources remains relatively consistent across all sensors, exceeding 50%, in particular during the winter months when there are significant anthropogenic contributions from biomass burning.

These findings provide valuable insights into the dynamics of local and regional sources of $PM_{2.5}$, highlighting their significant contributions to air quality variations in the monitored area. The ability of diurnal profile analysis to capture and adapt to specific PM effects underscores its effectiveness in understanding $PM_{2.5}$ variations.

6 Results in relation to the limit values and Air Quality Criteria

Low-cost sensors cannot replace the official reference instruments and they do not fulfil the requirements for equivalence with the reference method (EN 16450:2017, EN 12341:2014). This means that they can not be used for checking compliance with legally binding limit values.

The sensors can however give complementary information, providing indicative values of $PM_{2.5}$ and can be very useful to compare local differences of the $PM_{2.5}$ levels. Although sensor measurements cannot be evaluated with respect to legally binding limit values, they can provide valuable information of potential differences or agreement with the regulatory and assessment limits.

Figure 20 can be used to analyze cases where $PM_{2.5}$ concentration exceeds the daily guideline value for the nearest reference site in Tønsberg, revealing that 5% of the daily $PM_{2.5}$ data, equivalent to 37 out of 699 days, exceeds $15 \mu g m^{-3}$. As represented in Figure 2b, March 2022 stands out with the highest $PM_{2.5}$ levels and records the highest number of cases, totaling 14 days.

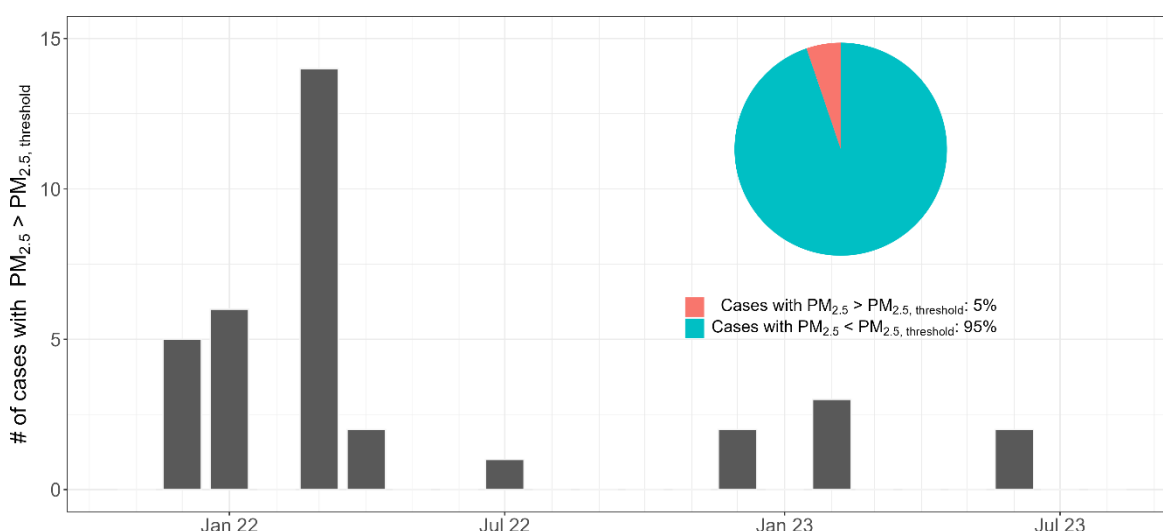


Figure 20: Time series of the daily number of occurrences with $PM_{2.5} > PM_{2.5, threshold} = 15 \mu g m^{-3}$ per month for Tønsberg. The pie chart includes the percentages of cases where $PM_{2.5}$ exceeded (or not) the air quality criteria for daily averages of $PM_{2.5}$.

Figure 21 provides a summary of the number of cases where $PM_{2.5}$ exceeded the daily guideline per month using the low-cost air quality sensors within Sandefjord's sensor network. The observed seasonal pattern closely mirrors that of the daily and monthly $PM_{2.5}$ concentrations. Table 5 provides information about the frequency and the concentrations of the days when $PM_{2.5}$ exceeds $15 \mu g m^{-3}$. In total, daily $PM_{2.5}$ is higher than the air quality criteria for ID425: 94 out of 637 days, ID426: 60 out of 637 days, ID427: 92 out of 594 monitored days, ID428: 85 out of 621 days, and ID450: 45 out of 589 days. The highest number of cases is recorded in December 2021, with some sensors reporting more than 20 days with $PM_{2.5}$ exceeding the daily guideline value. ID450 reports the lowest number of cases.

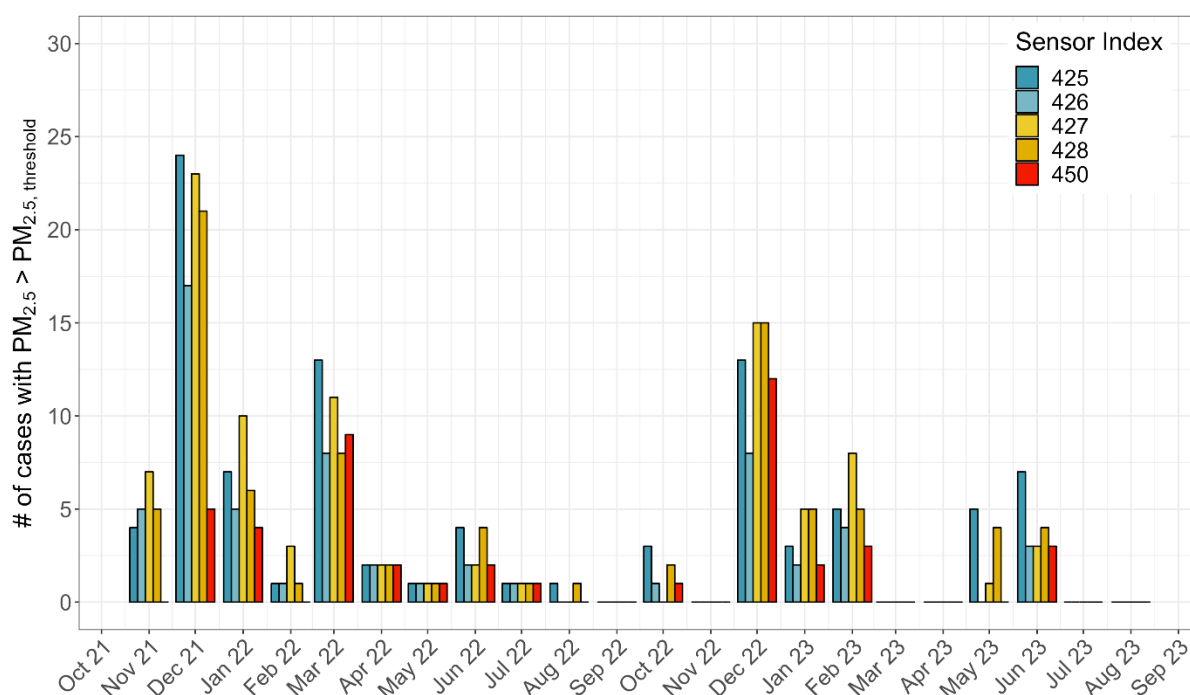


Figure 21: Time series of the daily number of occurrences with $PM_{2.5} > PM_{2.5, \text{threshold}} = 15 \mu\text{g m}^{-3}$ per month. Different colors correspond to sensors included in Sandefjord's air quality sensor network.

Table 5: Summary statistics for days with $PM_{2.5}$ exceeding the air quality criteria for daily averages ($15 \mu\text{g m}^{-3}$) for the entire measurement period. Days that $PM_{2.5}$ surpass the air quality criteria are classified into "Moderate", "High" and "Very High" levels following Table 2.

Sensor Index	Number of Days	Cases with $PM_{2.5} > 15 \mu\text{g m}^{-3}$		
		Number of Days	$PM_{2.5} (\mu\text{g m}^{-3})$	
			Mean	SD
425	637	93	22.4	7.8
		Moderate: 69, High: 24		
426	637	59	21.1	4.8
		Moderate: 45, High: 14		
427	594	91	22.9	7.9
		Moderate: 63, High: 28		
428	621	84	21.4	7.1
		Moderate: 65, High: 19		
450	589	45	20.1	4.5
		Moderate: 42, High: 3		



Figure 22: Bar plots for the Air Quality Index. The colored sections represent pollution classes described in Table 2. Different panels are for different seasons with DJF – Winter (December, January, February), MAM – Spring (March, April, May), JJA – Summer (June, July, August), and SON – Autumn (September, October, November).

The bar charts in Figure 22 display AQI on a seasonal basis for the Sandefjord area. Good air quality (class “Low”), represented by green areas, is the prevailing class in this region. The presence of “Moderate” and “High” AQI levels accounts for less than 10% of the total in spring, summer, and autumn (Figure 22 and Figure A10). However, a noticeable change occurs during the winter months, as there are days characterized by moderate and poor air quality. This shift is caused since daily average $\text{PM}_{2.5}$ concentrations are higher than $15 \mu\text{g m}^{-3}$ in several instances. This winter pattern is consistent across all air quality sensors (Figure A10). ID427 stands out as having the highest percentage of days with moderate and poor air quality, exceeding 30% in some cases, in contrast to the other sensors. Table 5 presents information regarding days categorized into “Moderate” and “High” classes. ID425, ID427 and ID428 show comparable number of days in the ‘Moderate’ level (63, 65 and 69, respectively). ID450 has 42 days classified as “Moderate” out of 45 days where the daily $\text{PM}_{2.5}$ exceeds the air quality criteria for daily averages, with 3 out of 45 days in the ‘High’ level. Figure A10 shows the monthly time series of AQI for each sensor. Each AQI class varies seasonally. For example, the number of ‘Moderate’ days is higher during the cold months due to the dominance of anthropogenic activities such as residential heating and lower in summer. December 2021, March 2022, and December 2022 depict the highest number of days in the “Moderate” and “High” pollution class. The AQI variations underscore the impact of specific local factors and sources on air quality during the winter season, leading to the observed variations in AQI levels. As mentioned before, the main source in December 2021 and 2022 is wood burning, while in March 2022 it is a long-range transport episode.

7 General conclusions

In an urban setting where regulatory stations are limited or absent, the use of low-cost sensors for monitoring air quality can yield valuable insights into the current air quality conditions. These sensors have shown significant promise in measuring air pollutants, particularly PM_{2.5}. This report discusses the PM_{2.5} concentrations in Sandefjord, Norway, spanning from November 2021 to September 2023. The analysis of PM_{2.5} is conducted at various time intervals, offering information on air quality patterns over different timeframes and providing information on the local and regional factors influencing PM_{2.5} variability. The key findings of this report can be summarized as follows:

- Sensor reliability is high, with consistent PM_{2.5} measurements and similar variation over time. Occasional extreme PM_{2.5} is attributed to local contributions with higher values observed during colder months, or specific PM events.
- Sensors are not equivalent to reference instruments, and their readings can only be considered as indicative. However, indicative measurements offer information that can guide policy measures aimed at reducing air pollution.
- PM_{2.5} exhibits two notable peaks during the day throughout all seasons, except for summer when a nearly flat pattern is observed. The significance and magnitude of these peaks are influenced by a) the time of day the peak occurs (morning vs. evening) and b) the varying extent of local contribution.
- PM_{2.5} is well correlated with air temperature during specific months and times of the day. An increase in PM_{2.5} during lower temperature conditions suggests the dominance of residential heating-based activities.
- Sensors' PM_{2.5} measurements closely align with those from the reference station in Tønsberg, located approximately 18 kilometers from Sandefjord, particularly during non-polluted hours.
- Local sources account for more than 50% of PM_{2.5}, especially during months with potential anthropogenic contributions.
- The air quality in Sandefjord is good during most of the year. However, elevated PM_{2.5} concentrations are recorded during wintertime (e. g. December 2021 and 2022) and during specific events, such as the PM long-range transport event in March 2022.

8 References

- [1] Moltchanov, S., Levy, I., Etzion, Y., Lerner, U., Broday, D. M., Fishbain, B., On the feasibility of measuring urban air pollution by wireless distributed sensor networks. *Sci. Total. Environ.* 2015, 502, 537–547, <https://doi.org/10.1016/j.scitotenv.2014.09.059>.
- [2] Hassani, A., Schneider, P., Vogt, M., Castell, N., Low-cost particulate matter sensors for monitoring residential wood burning. *Environ. Sci. Technol.* 2023, 57, 40, 15162–15172, <https://doi.org/10.1021/acs.est.3c03661>.
- [3] Petters, M. D., Kreidenweis, S. M., A single parameter representation of hygroscopic growth and cloud condensation nucleus activity, *Atmos. Chem. Phys.* 2007, 7, 1961–1971, <https://doi.org/10.5194/acp-7-1961-2007>.
- [4] Crilley, L. R., Shaw, M., Pound, R., Kramer, L. J., Price, R., Young, S., Lewis, A. C., Pope, F. D., Evaluation of a low-cost optical particle counter (Alphasense OPC-N2) for ambient air monitoring, *Atmos. Meas. Tech.* 2018, 11, 709–720, <https://doi.org/10.5194/amt-11-709-2018>.
- [5] Crilley, L. R., Singh, A., Kramer, L. J., Shaw, M. D., Alam, M. S., Apte, J. S., Bloss, W. J., Hildebrandt Ruiz, L., Fu, P., Fu, W., Gani, S., Gatari, M., Ilyinskaya, E., Lewis, A. C., Ng'ang'a, D., Sun, Y., Whitty, R. C. W., Yue, S., Young, S., Pope, F. D., Effect of aerosol composition on the performance of low-cost optical particle counter correction factors, *Atmos. Meas. Tech.* 2020, 13, 1181–1193, <https://doi.org/10.5194/amt-13-1181-2020>.
- [6] Schneider, P., Vogt, M., Haugen, R., Hassani, A., Castell, N., Dauge, F. R., Bartonova, A., Deployment and evaluation of a network of open low-cost air quality systems. *Atmosphere* 2023, 14 (3), 540, <https://doi.org/10.3390/atmos14030540>.
- [7] Liu, H.Y., Schneider, P., Haugen, R., Vogt, M., Performance assessment of a low-cost PM_{2.5} sensor for a near four-month period in Oslo, Norway. *Atmosphere* 2019, 10 (2), 41, <https://doi.org/10.3390/atmos10020041>.
- [8] Hamer, P. D., Fjæraa, A.-M., Tarassón, L., Soares, J., Meleux, F., Colette, A., Ung, A., Raux, B., Kuenen, J. Copernicus Atmosphere Monitoring Service Interim Annual Assessment Report on European Air Quality in 2022, Copernicus Atmosphere Monitoring Service (CAMS) report, https://policy.atmosphere.copernicus.eu/reports/CAMS271_2021SCx_D1.1.1_202306_2022_Interim_Assessment_Report_v1.pdf
- [9] Tsyro, S., Schulz, M., Mortier, A., Valdebenito, A., Benedictow, A., Timmerman, R., Kranenburg, R., High PM₁₀ levels: episode of 20-27 March 2–22 - CAMS2_71 episode analysis report N°02 in 2022, CAMS71_D3.2.1-2022-2-B_20-27MarchEpisode (CAMS), https://policy.atmosphere.copernicus.eu/reports/CAMS2-71_PM10_episode_20-27March2022_final.pdf
- [10] Kukkonen, J., López-Aparicio, S., Segersson, D., Geels, C., Kangas, L., Kauhaniemi, M., Maragkidou, A., Jensen, A., Assmuth, T., Karppinen, A., Sofiev, M., Hellén, H., Riikonen, K., Nikmo, J., Kousa, A., Niemi, J. V., Karvosenoja, N., Santos, G. S., Sundvor, I., Im, U., Christensen, J. H., Nielsen, O.-K., Plejdrup, M. S., Nøjgaard, J. K., Omstedt, G., Andersson, C., Forsberg, B., Brandt, J., The influence of residential wood combustion on the concentrations of PM_{2.5} in four Nordic cities, *Atmos. Chem. Phys.* 2020, 20, 4333–4365, <https://doi.org/10.5194/acp-20-4333-2020>.

- [11] Lopez-Aparicio, S., Grythe, H., Evaluating the effectiveness of a stove exchange program on PM_{2.5} emission reduction. *Atmos. Environ.* 2020, 231, 117529, <https://doi.org/10.1016/j.atmosenv.2020.117529>.
- [12] Gómez-Losada, Á., Pires, J.C.M., Pino-Mejías, R., Characterization of background air pollution exposure in urban environments using a metric based on Hidden Markov Models. *Atmos. Environ.* 2016, 127, 255–261. <https://doi.org/10.1016/j.atmosenv.2015.12.046>.
- [13] Frederickson, L. B., Sidaraviciute, R., Schmidt, J. A., Hertel, O., Johnson, M. S., Are dense networks of low-cost nodes really useful for monitoring air pollution? A case study in Staffordshire. *Atmos. Chem. Phys.* 2022, 22, 13949–13965, <https://doi.org/10.5194/acp-22-13949-2022>.
- [14] Byrne, R., Ryan, K., Venables, D., Wenger, J., Hellebust, S., Highly local sources and large spatial variations in PM_{2.5} across a city: evidence from a city-wide sensor network in Cork, Ireland. *Environ. Sci.: Atmos.* 2023, 3, 919–930, <https://doi.org/10.1039/D2EA00177B>.
- [15] Kosmopoulos, G., Salamalikis, V., Matrali, A., Pandis, S.N., Kazantzidis, A., Insights about the sources of PM_{2.5} in an urban area from measurements of a low-cost sensor network. *Atmosphere* 2022, 13, 440. <https://doi.org/10.3390/atmos13030440>.
- [16] Diamantopoulou, M., Skyllakou, K., Pandis, S. N., Estimation of local and long-range contribution to particulate matter levels using continuous measurements in a single urban background site. *Atmos. Environ.*, 2016, 134, 1–9, <https://doi.org/10.106/j.atmosenv.2016.0.015>.

Appendix A

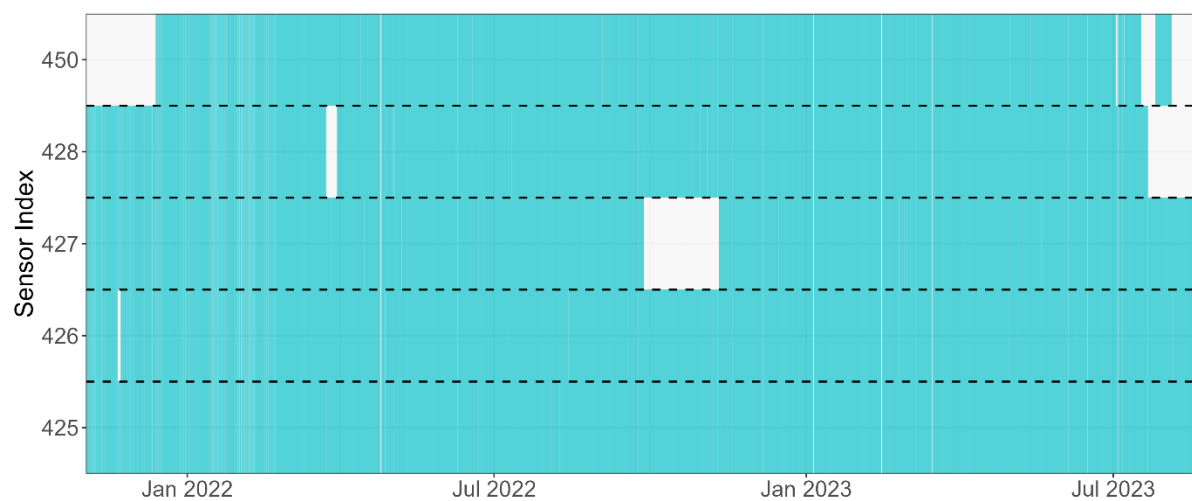


Figure A1: Data coverage for the individual air quality sensors. The blank areas correspond to non-available measurements.

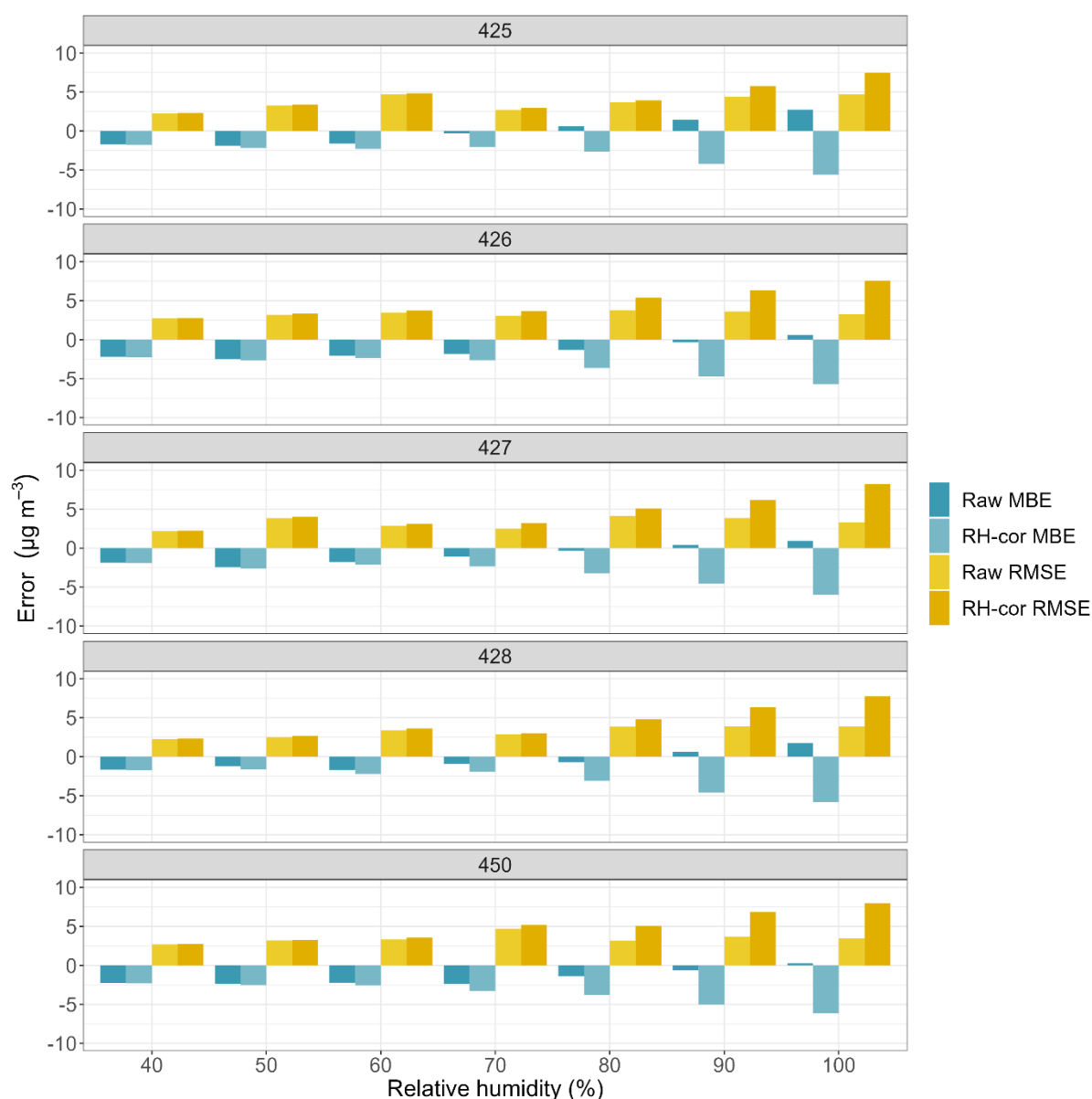


Figure A2: Bar plots of the systematic (Mean Bias Error, MBE) and dispersion (Root Mean Square Error, RMSE) errors between raw and humidity-corrected LCS $PM_{2.5}$ against reference $PM_{2.5}$ in Tønsberg for different relative humidity cases. The horizontal axis is in units of % and the vertical axis is in units of $\mu g m^{-3}$. The Raw and RH-cor in the color key correspond to the initially measured and humidity-corrected (based on **Error! Reference source not found.**) LCS $PM_{2.5}$ concentrations. MBE and RMSE are defined as, $MBE = \frac{\sum_{i=1}^n (LCS PM_{2.5} - Reference PM_{2.5})}{n}$ and $RMSE = \sqrt{\frac{\sum_{i=1}^n (LCS PM_{2.5} - Reference PM_{2.5})^2}{n}}$. LCS underestimate (overestimate) reference $PM_{2.5}$ for negative (positive) MBE. High RMSE values indicate a great dispersion between LCS and reference $PM_{2.5}$.

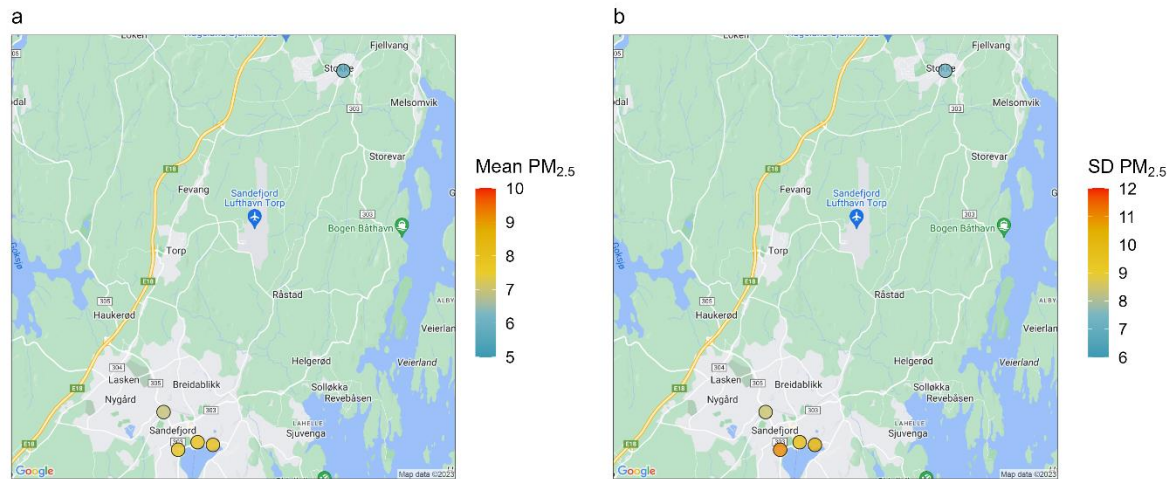


Figure A3: Spatial distribution of $PM_{2.5}$ a) average and b) standard deviation (SD). The color key is in units of $\mu g m^{-3}$.



Figure A4: Spatial distribution of monthly $PM_{2.5}$ for the Sandefjord air quality sensors. Warm/cold colors are for high/low $PM_{2.5}$ concentrations. Missing data cases are drawn with grey circles. A monthly average is calculated assuming data completeness of 75% (more than 75% of available daily measurements per month).



Figure A5: Spatial distribution of diurnal $\text{PM}_{2.5}$ for the Sandefjord air quality sensors. Warm/cold colors are for high/low $\text{PM}_{2.5}$ concentrations. Missing data cases are drawn with grey circles.

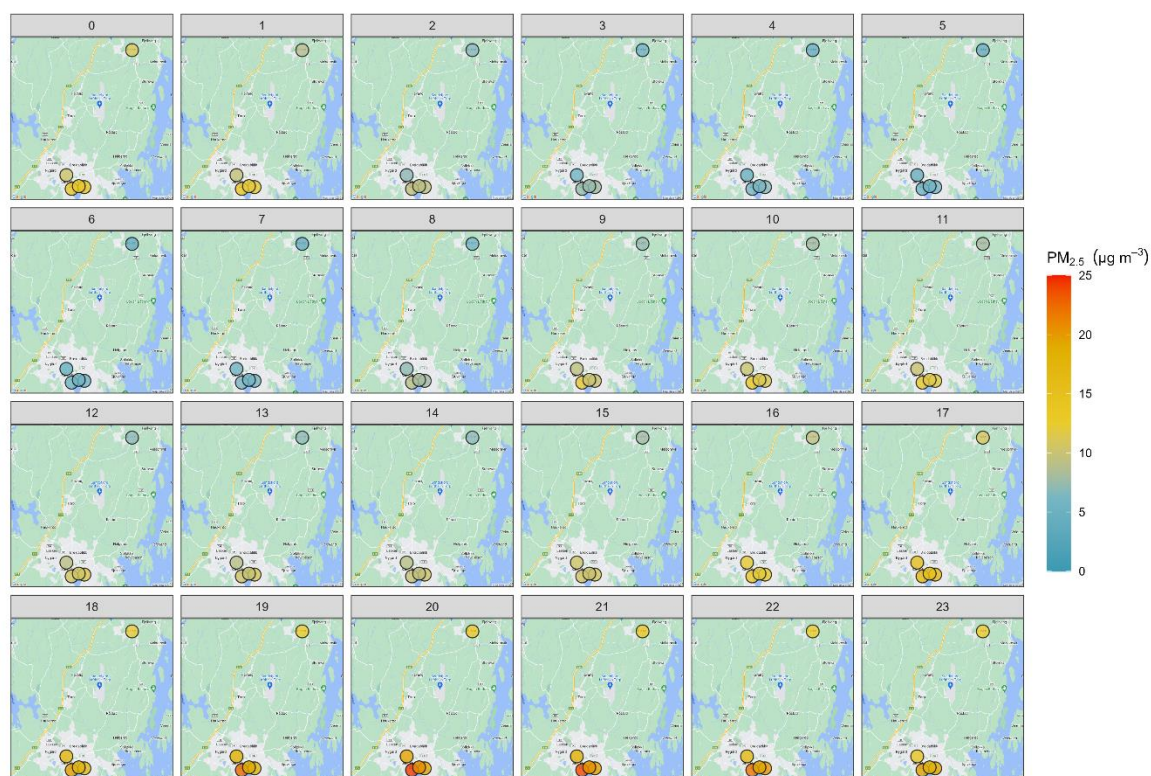


Figure A6: Spatial distribution of diurnal $PM_{2.5}$ in winter (DJF) for the Sandefjord air quality sensors. Warm/cold colors are for high/low $PM_{2.5}$ concentrations. Missing data cases are drawn with grey circles.



Figure A7: Spatial distribution of diurnal $PM_{2.5}$ in spring (MAM) for the Sandefjord air quality sensors. Warm/cold colors are for high/low $PM_{2.5}$ concentrations. Missing data cases are drawn with grey circles.



Figure A8: Spatial distribution of diurnal PM_{2.5} in summer (JJA) for the Sandefjord air quality sensors. Warm/cold colors are for high/low PM_{2.5} concentrations. Missing data cases are drawn with grey circles.

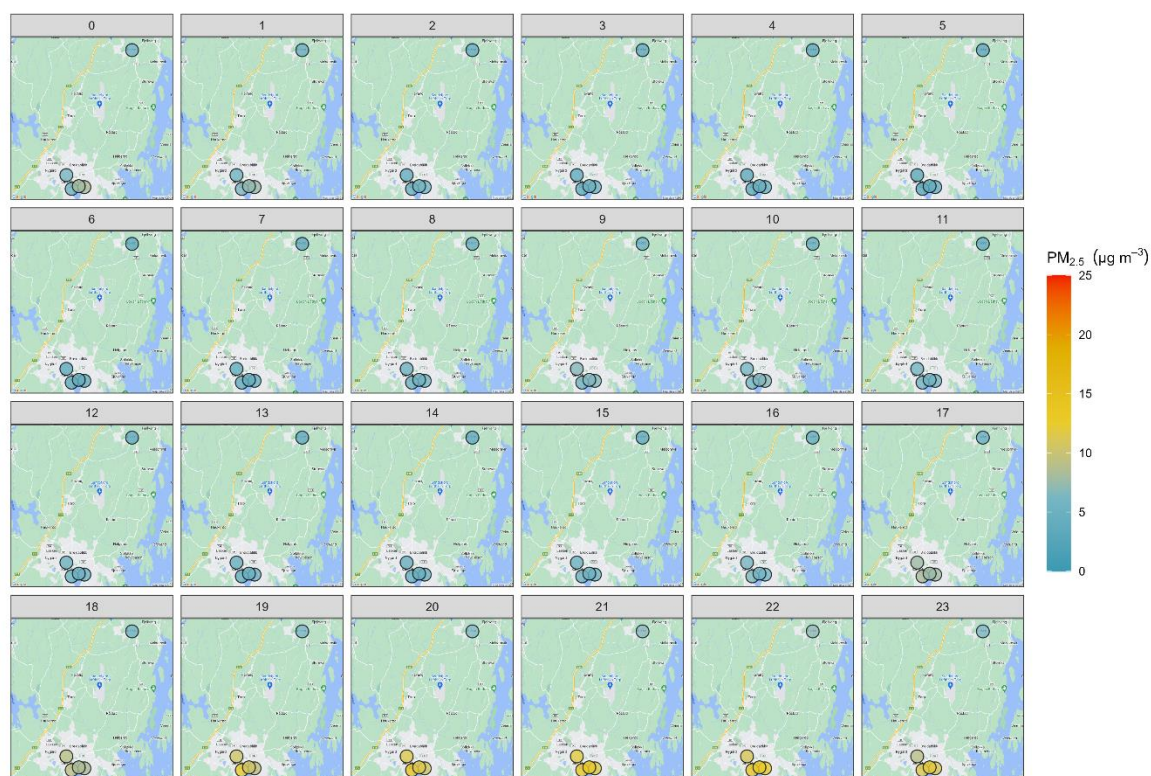


Figure A9: Spatial distribution of diurnal $\text{PM}_{2.5}$ in autumn (SON) for the Sandefjord's air quality sensors. Warm/cold colors are for high/low $\text{PM}_{2.5}$ concentrations. Missing data cases are drawn with grey circles.

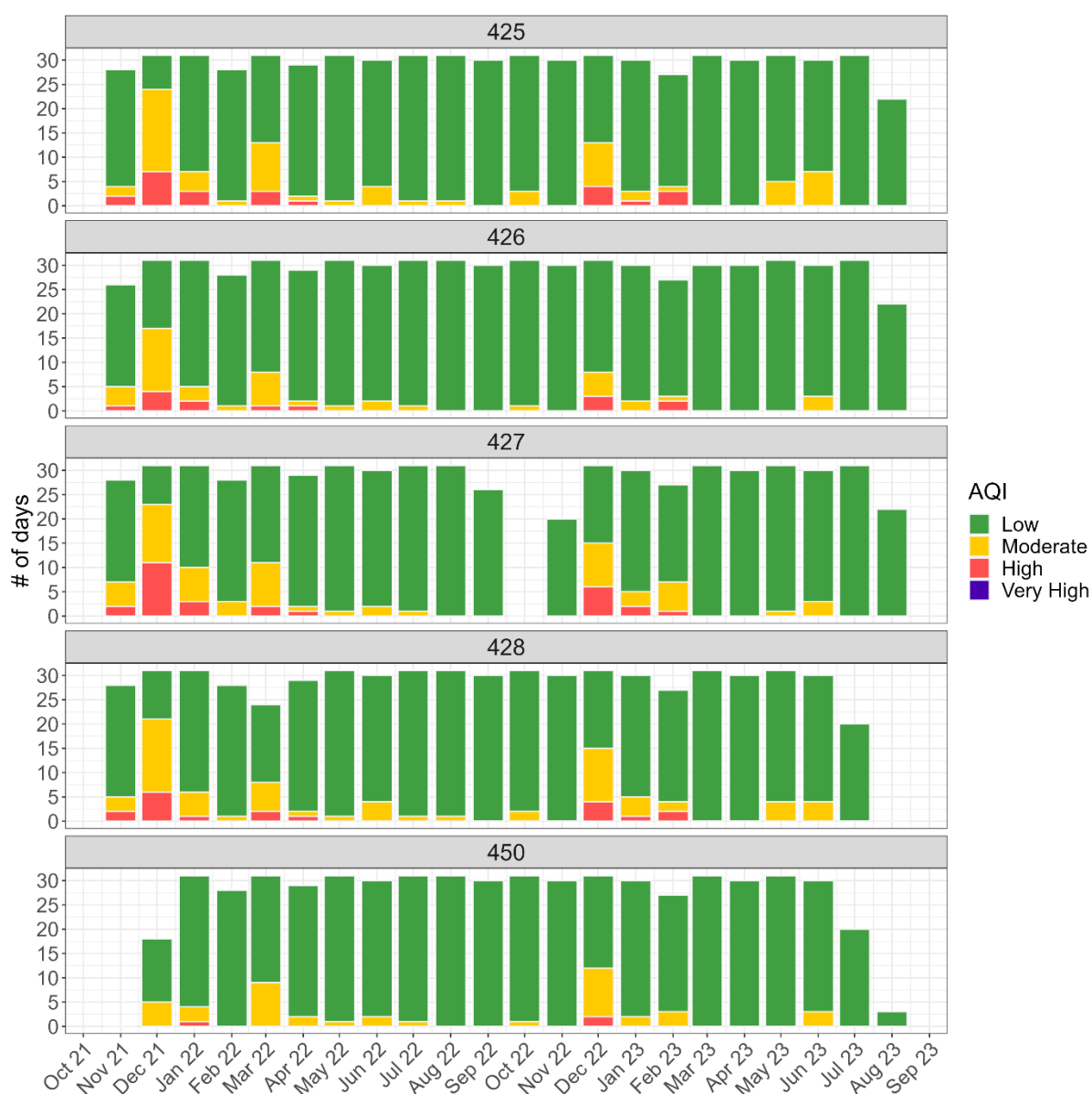


Figure A10: Monthly bar plots of the Air Quality index for the five sensors. The vertical axis represents the number of days in each month. Different colors correspond to different AQI levels (Table 2).



The climate and environmental research institute NILU is an independent, non-profit research institution established in 1969. Through its research NILU increases the understanding of atmospheric composition, climate change, air quality, environmental contaminants, health effects, sustainable systems, circular economy, and digitalisation. Based on its research, NILU markets integrated services and products within analysing, monitoring and consulting. NILU is concerned with increasing public awareness about climate change and environmental pollution.